1983MNRAS.204..415C

Mon. Not. R. astr. Soc. (1983) **204**, 415–431 and *Microfiche* MN204/1

Three-dimensional structure of the Crab Nebula

David H. Clark *Space and Astrophysics Division, Rutherford Appleton Laboratory, Chilton, Didcot, Oxfordshire*

Paul Murdin, Roger Wood and Roberto Gilmozzi* *Royal Greenwich Observatory, Herstmonceux Castle, Hailsham, East Sussex*

John Danziger *European Southern Observatory, Karl Schwarzchild Strasse 2, D-8046, Garching-bei-Munchen, Federal Republic of Germany*

Andrew W. Furr *Astronomy Centre, University of Sussex, Falmer, Brighton, East Sussex*

Received 1983 January 24; in original form 1982 October 20

Summary. Radial velocity observations from the Crab Nebula are used to investigate its three-dimensional properties. In the standard model, it consists of a thick, hollow shell, with synchrotron emission from within. We show that the thick shell is composed of bright inner and faint outer components surrounded by a higher velocity halo. Filaments are generally circumferential, but radial 'spokes' link the inner and outer shells. There are spectral differences between the two extremities of the thick shell. The Crab Nebula's synchrotron emission is confined within the shell system with a sharp discontinuity in brightness at the bright inner shell.

1 Introduction

Previous investigations of the dynamics of the Crab Nebula have been based on the radial velocity observations of Mayall (1962), Woltjer (1958), Münch (1958) and Trimble (1968) and proper motion measurements by Duncan (1939), Deutsch & Lavdovsky (1940), Trimble (1968) and Wyckoff & Murray (1977). Trimble's work has become the standard model in which it is supposed that the nebula is a prolate spheroid, at distance ~ 2 kpc. The nebula's expansion velocity gives an outburst date of AD 1140, thus requiring post-outburst acceleration to relate the Crab Nebula to the supernova of AD 1054. Trimble's observations suggested that the Crab has a thick shell.

Earlier observations were restricted to selected positions within the nebula. The observations reported here cover the whole nebula in a systematic way, resulting in an order-of-

* Present address: Istituto di Astrofisica Spaziale, C.P. 67, 00044 Frascati/9421197, Italy.

magnitude increase in the available velocity data compared with earlier work: they both confirm and extend the accepted model.

2 Observations and data reduction

Observations were made during 1977 November (supplemented in 1979 and 1982) using the RGO spectrograph and image photon counting system (IPCS) attached to the 3.9-m Anglo-Australian telescope. The IPCS was operated in two-dimensional mode, with resolution of 4.7 arcsec along the slit and 0.46 Å in dispersion. The spectral resolution corresponds to a velocity resolution of about $30\,\mathrm{km\,s^{-1}}$ at 5000 Å. Radial velocities were estimated from displacements of the λ 5007 [O III] line, with wavelength calibration achieved using a copper–argon arc.

The spectrograph slit was positioned east–west and 100-s duration exposures were taken at each of 28 declination positions, separated by 10 arcsec, with slit width 1 arcsec so that 10 per cent of the nebula surface was sampled. By this process 1800 independent spectra were obtained over the face of the nebula forming a regular grid of pixels spaced 4.7 arcsec in right ascension and 10 arcsec in declination (equivalent to 0.05×0.1 pc at a distance of 2 kpc).

From each of the 1800 spectra, the red/blueshift of the [O III] λ 5007 line was estimated (within the errors quoted) and converted to a velocity of recession (or approach) with respect to the rest wavelength. In most cases several features with different red/blueshifts were noted at the same point. It proved possible to distinguish redshifted λ 4959 from blueshifted λ 5007 by inspection of the relative intensities of the lines, and we are confident that the velocities measured are negligibly contaminated by this ambiguity.

More than 300 velocity estimates are tabulated in Tables 1 and 2 (*Microfiche* MN204/1), where bright features (those having peak intensity greater than 100 counts in 100-s exposure) are marked with an asterisk. The velocity map pixels are identified by X (column number) and Y (row number) coordinates where X ranges from 1 to 66, defining the right ascension of a pixel, and Y ranging from 1 to 28, defining the declination. The origin of this system is the centre of the pixel in the north-eastern corner of the map, and positions on the sky can be located by reference to the pulsar at pixel (39, 14) and its equinox 1950.0 coordinates. Hence the centre of any pixel (X, Y) is given by

$$\mathrm{RA}\,(1950.0) = 05^{\mathrm{h}}\,31^{\mathrm{m}}\,32^{\mathrm{s}} - (X-39) \times 4.7\ \mathrm{arcsec}$$
$$\mathrm{Dec}\,(1950.0) = +21^\circ\,58'\,55'' - (Y-14) \times 10\ \mathrm{arcsec}.$$

The velocity data are summarized in the 'colourgraphs' of Plate 1. The total data sets and bright feature data sets are depicted separately, for far- and near-side of the nebula. Where several red or blueshift velocity values were obtained for a single pixel, the largest was used in the colourgraph.

The average velocity of 3147 velocity estimates is $-89\,\mathrm{km\,s^{-1}}$. There are 20 per cent more estimates of blueshifts than of redshifts. The mean of the average blueshifts and the average redshifts is $-20\,\mathrm{km\,s^{-1}}$. Compared with the maximum expansion speeds in the data set of Tables 1 and 2 of about $1800\,\mathrm{km\,s^{-1}}$, the systematic centre-of-light velocity of the nebula is insignificant (Trimble 1968).

3 Structure of the Crab Nebula

3.1 VELOCITY ELLIPSE

A series of spectra obtained every 4.7 arcsec on an east–west line through the centre of the nebula is shown in Fig. 1(a), which displays both [O III] lines, $\lambda\lambda$ 5007, 4959. The velocity ellipse evident here (and at all other slit positions) is characteristic of emission originating

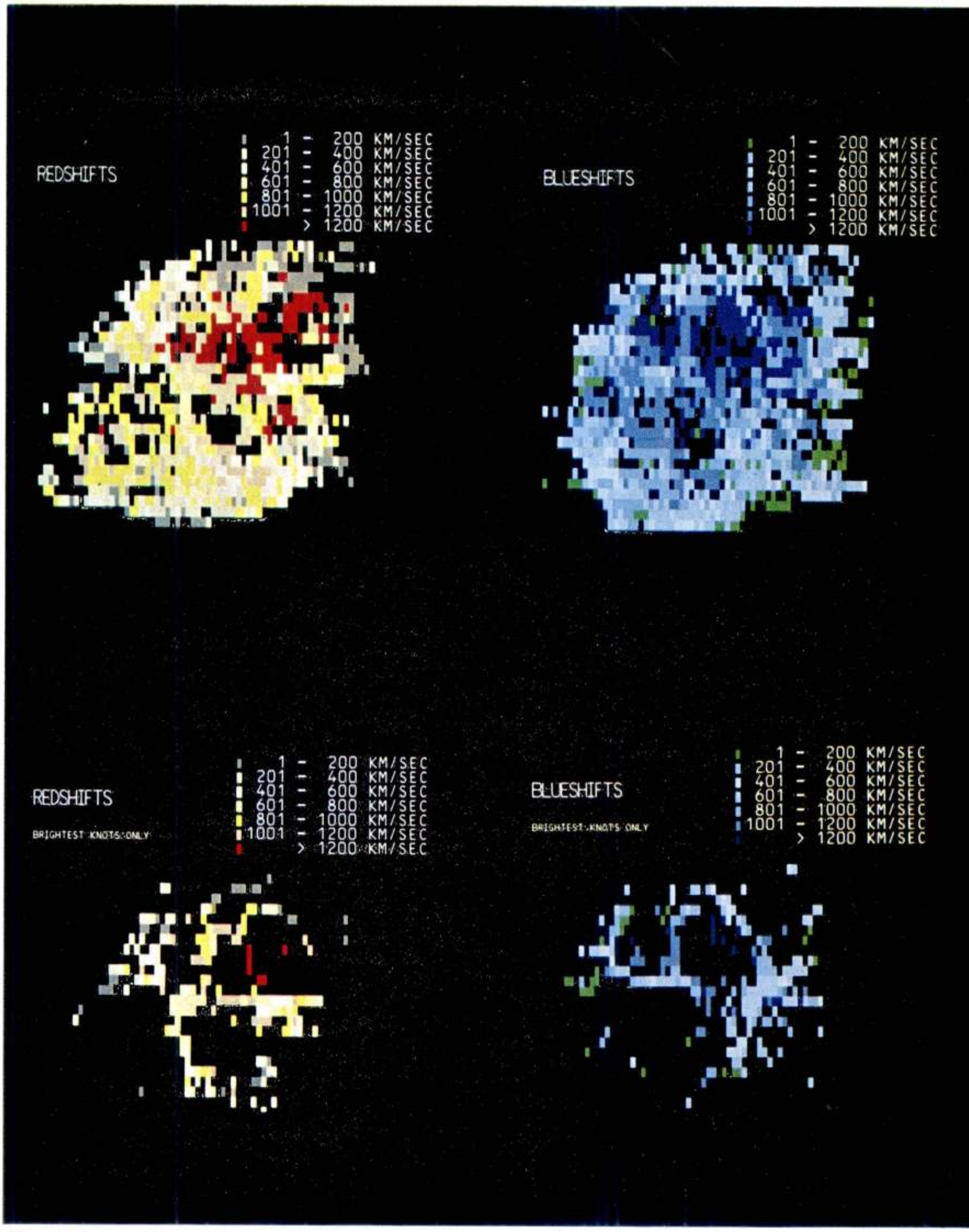

Plate 1. These colourgraphs, constructed from the data in the tables, show the velocity structure of the Crab Nebula. The blue pictures show the approaching (near-side) of the nebula: the red pictures show the receding (far-side). In the upper pair of pictures all data points are shown: the lower pair contain data from the brightest knots only. Where several values of radial velocity were obtained for a single pixel only the largest has been used. Note the congregation of the highest red- and blueshifts in the upper right (north-west) quadrant.

[*facing page* 416]

in an expanding shell of material. The spread in radial velocity about the maxima arises because the shell has a certain thickness in the line-of-sight. The ellipse seen in Fig. 1(a) can be modelled as two concentric thin surfaces representing the inner and outer boundaries of this thick shell, within which most of the emission lies. The inner surface is expanding at $720\,\mathrm{km\,s^{-1}}$ relative to the centre, the outer at $1800\,\mathrm{km\,s^{-1}}$. The relative thickness of the shell along the line-of-sight is measured by the ratio of inner and outer diameters which is 0.40. Alternatively the thickness of the shell may be perceived from the extent of the emission along the slit. The inner diameter is 135 arcsec, the outer 340 arcsec and the thickness of the shell transverse to the line-of-sight is measured by the ratio of these numbers and is also 0.40.

The outer boundary to the second shell cannot be interpreted literally. Murdin & Clark (1981) have shown photographic evidence for a faint red (Hα?) halo around the Crab Nebula. Dennefeld (1983) has discovered faint features in his near-infrared spectra and attributes them to high velocity filaments at $+3880$ and $+4940\,\mathrm{km\,s^{-1}}$. In our spectra there is faint $\lambda\,5007$ emission (most readily visible on the far side of the nebula where it is not confused by the redshifted $\lambda\,4959$ line) which lies beyond the $1800\,\mathrm{km\,s^{-1}}$ boundary. In Fig. 1(a) emission at $+1700\,\mathrm{km\,s^{-1}}$ can be seen 10 spectra from the top (upper right-hand corner). The projection factor means that this emission represents an expansion velocity in excess of $\sim 2300\,\mathrm{km\,s^{-1}}$.

Fig. 1(b) shows evidence for emission from high velocity material beyond the bright outline of the nebula. The composite formed by summing all the individual spectra in the east–west section through the pulsar is shown in the middle. At the bottom is a sky spectrum constructed from contributions taken from positions along an extension of the minor axis of the nebula about 1.5 arcmin outside the boundary and which appear to have no emission: in any case any emission in such places is likely to have zero velocity because it lies at the edge of the nebula. The top spectrum is then the difference between these two (representing the filamentary spectrum on top of the synchrotron continuum) and shows extended emission to the red of the $\lambda\,5007$ line to $+3600\,\mathrm{km\,s^{-1}}$ and to the blue of the $\lambda\,4959$ line to $-2400\,\mathrm{km\,s^{-1}}$.

Thus, if the same relationship between radial velocity and line-of-sight depth holds for this materal as for the shells, we confirm the existence of a high velocity halo around the Crab Nebula extending to at least twice the radius of the outer shell.

3.2 VELOCITY SECTIONS

Figs 2 and 3 show respectively red and blueshift 'velocity sections' through the Crab Nebula and Figs 4 and 5 similar data for the bright features only. Each velocity section is a picture of the spatial distribution of points within a $100\,\mathrm{km\,s^{-1}}$ velocity band ($200\,\mathrm{km\,s^{-1}}$ for brightest points only). On the assumption that radial distance along the line-of-sight is proportional to the radial velocity, each velocity sheet may be considered to be a cross-section of the nebula at a certain distance along the line-of-sight, with the largest blueshifts representing the nearest section. If the nebula is 2 kpc away, the pixels on the sky measure 1.4 by 2.9×10^{12} km (0.05×0.1 pc) and the $100\,\mathrm{km\,s^{-1}}$ velocity sheets chosen are separated by 2.5×10^{12} km (0.08 pc). Hence the spatial resolution selected for the line-of-sight is very nearly the same as that on the sky. The data 'brick' is of dimension $66 \times 28 \times 32$ ($3.0 \times 2.6 \times 2.6$ pc).

The correctness of the topology of the data brick is confirmed by radio polarization measurements at high resolution (Swinbank 1980) which demonstrate how the front filaments of the nebula, as defined by the present dataset, depolarize the synchrotron emission from within the shell.

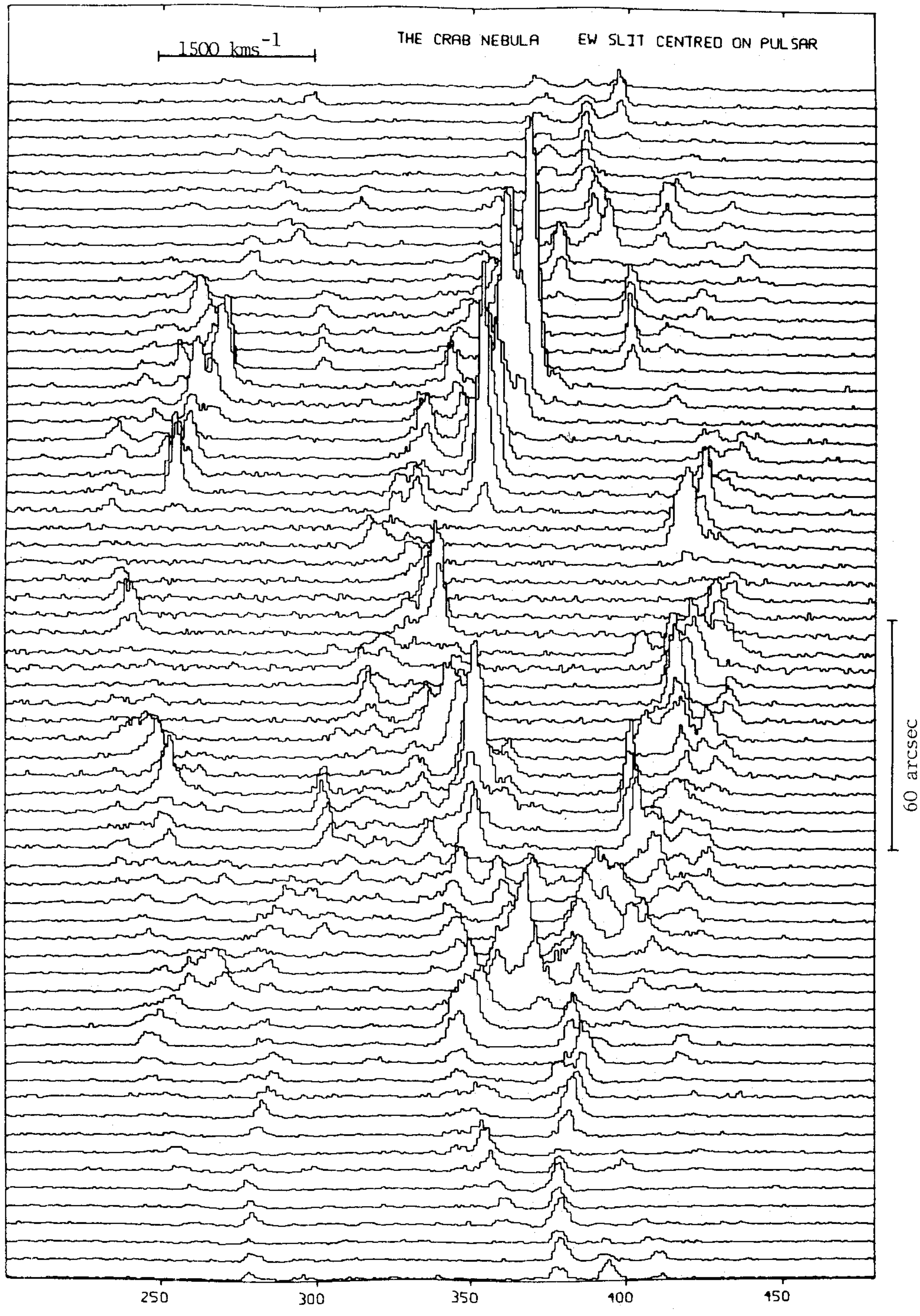

1500 kms^{-1}
THE CRAB NEBULA EW SLIT CENTRED ON PULSAR
60 arcsec
250
300
350
400
450
CHANNEL NUMBER

Figure 1(a)

The thick shell of the Crab Nebula may be seen in Figs 2 and 3. The hollowness of the shell is demonstrated by the absence of emission near $X = 39$, $Y = 14$ (the pulsar) in the low velocity ($|V_r| < 400 \text{ km s}^{-1}$) sections. The velocity sections confirm the thickness of the shell derived in Section 3.1. The existence of the hollow centre is also clearly seen in Figs 6 and 7 where the radial distances of pixels from the pulsar are plotted against the velocities present in those pixels. Except for one point at 60 km s^{-1} (from pixel $X = 31$, $Y = 11$) there are no low velocity points close to the nebula centre. (We do note, however, that Trimble 1968 found *three* isolated knots within this hollow space. The knots were chosen to be measurable for proper motions and were small; the other two may have been stepped over by the 10 arcsec sampling in declination. Such knots are clearly rare.) These diagrams also confirm the evident thickness of the nebula's shell: however, the double structure is not seen here since all points are treated with equal weight, but runs of points, representing near-radial filaments, can sometimes be perceived.

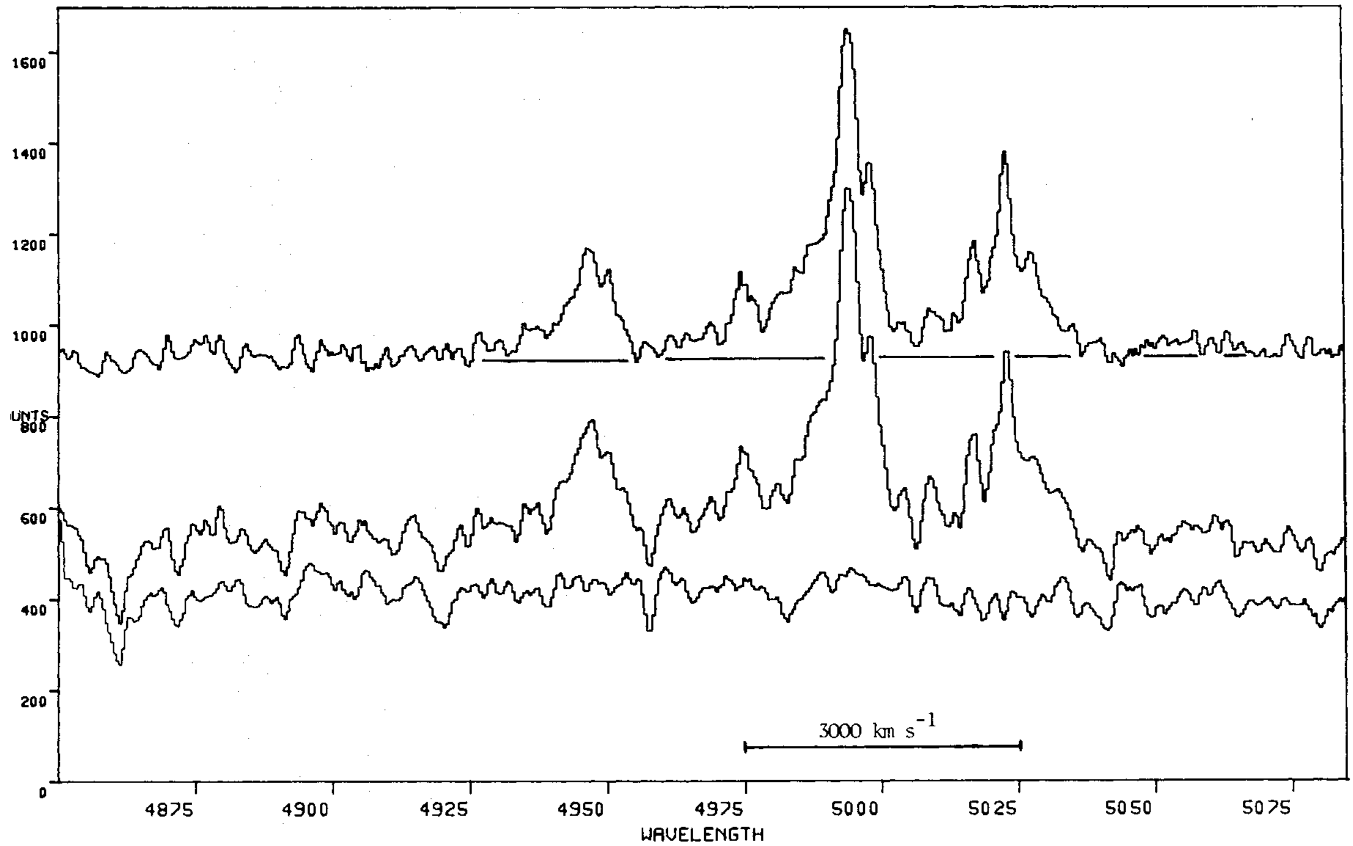

(b)

Figure 1. (a) Velocity ellipse of the [O III] lines shown as 68 spectra of intensity versus channel number. Each spectrum is from an increment of length 4.7 arcsec of a long slit, oriented east–west and centred on the pulsar. East is at the bottom and the pulsar is in the spectrum 35 from the bottom. Wavelength increases to the right, each channel being 0.5 Å (30 km s^{-1}) wide, with the rest wavelength of λ 5007 falling in channel 377. (b) The data in (a) have been summed (centre spectrum). A sky spectrum (lower spectrum) has been formed from an equal area, centred away from the nebula about 1.5 arcmin north-east along the minor axis. The difference (top spectrum, offset 800 counts from the base) represents filamentary emission on the synchrotron continuum. Interpolating from assumed continuum positions at about 4910 and 5075 Å gives the base level shown. Filamentary emission extends to 5065 Å ($+3600 \text{ km s}^{-1}$ if identified with λ 5007) and 4920 Å (-2400 km s^{-1} if identified with λ 4959).

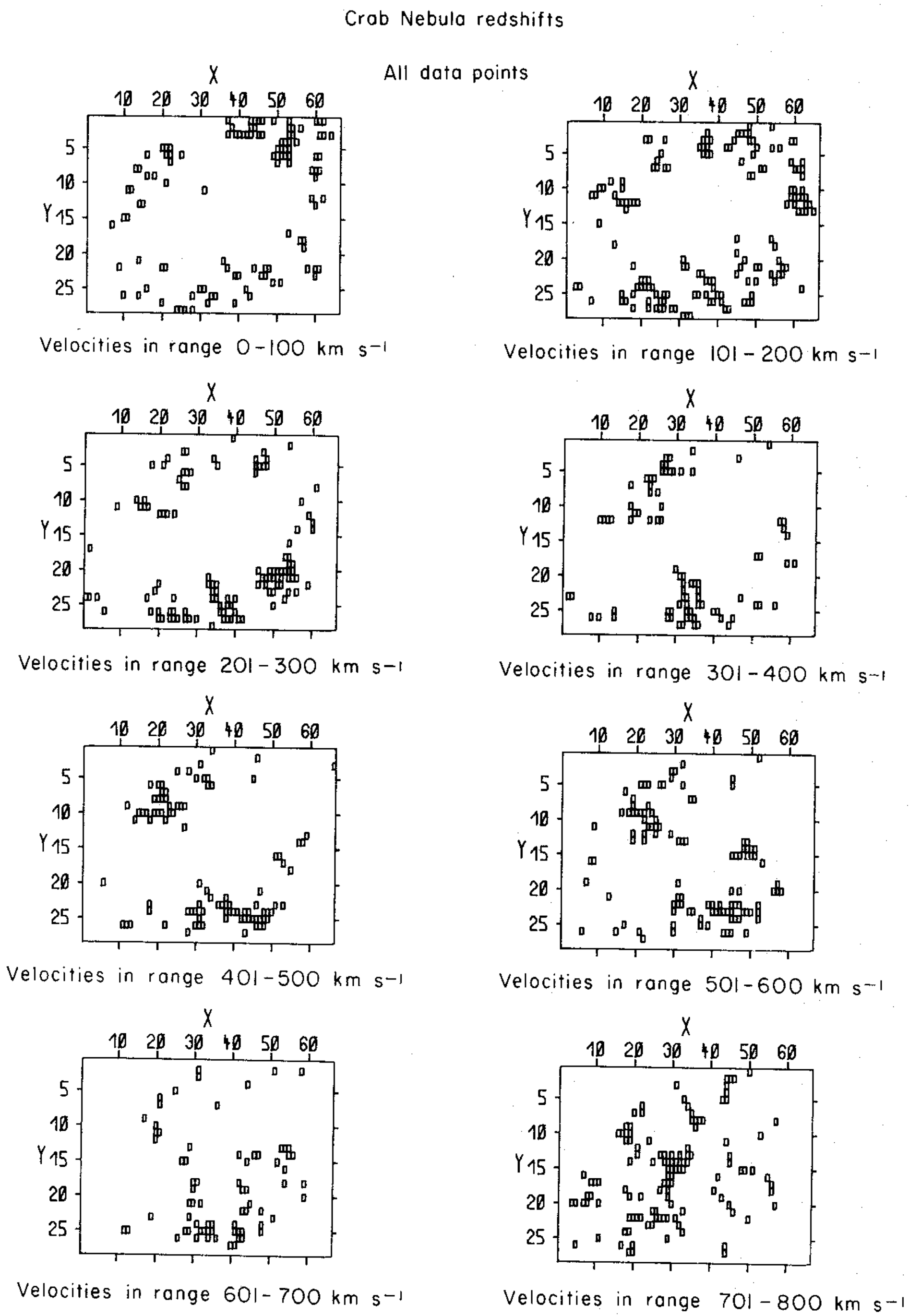

Figure 2. Sections through the Crab Nebula in redshifted velocity space. North-east is upper left. The $100\,\mathrm{km\,s^{-1}}$ sampling has about the same resolution as the declination pixels (~ 0.10 pc). Filaments are most prominent in the $701-800\,\mathrm{km\,s^{-1}}$ section, lying between the inner and outer shell, which shows that filaments run mostly circumferentially around the Crab Nebula, but the 101–200 and 201–300 $\mathrm{km\,s^{-1}}$ sections shows that the filaments are angled across the thickness of the shell [e.g. the filament which starts near ($X = 10$, $Y = 10$, $V = 101-200$) and runs to ($X = 25$, $Y = 12$, $V = 201-300$)].

The diagrams in Fig. 8 were also constructed from the velocity data. They show cross-sections (perpendicular to the plane of the sky) through the nebula. Taking the major axis to be at position angle 135° and the minor axis at 225° (with the axis intersecting at the pulsar), the velocities and radial distances from the pulsar are plotted for those pixels lying on the axes or up to two pixels either side. Using the expansion age of 840 yr, consistent

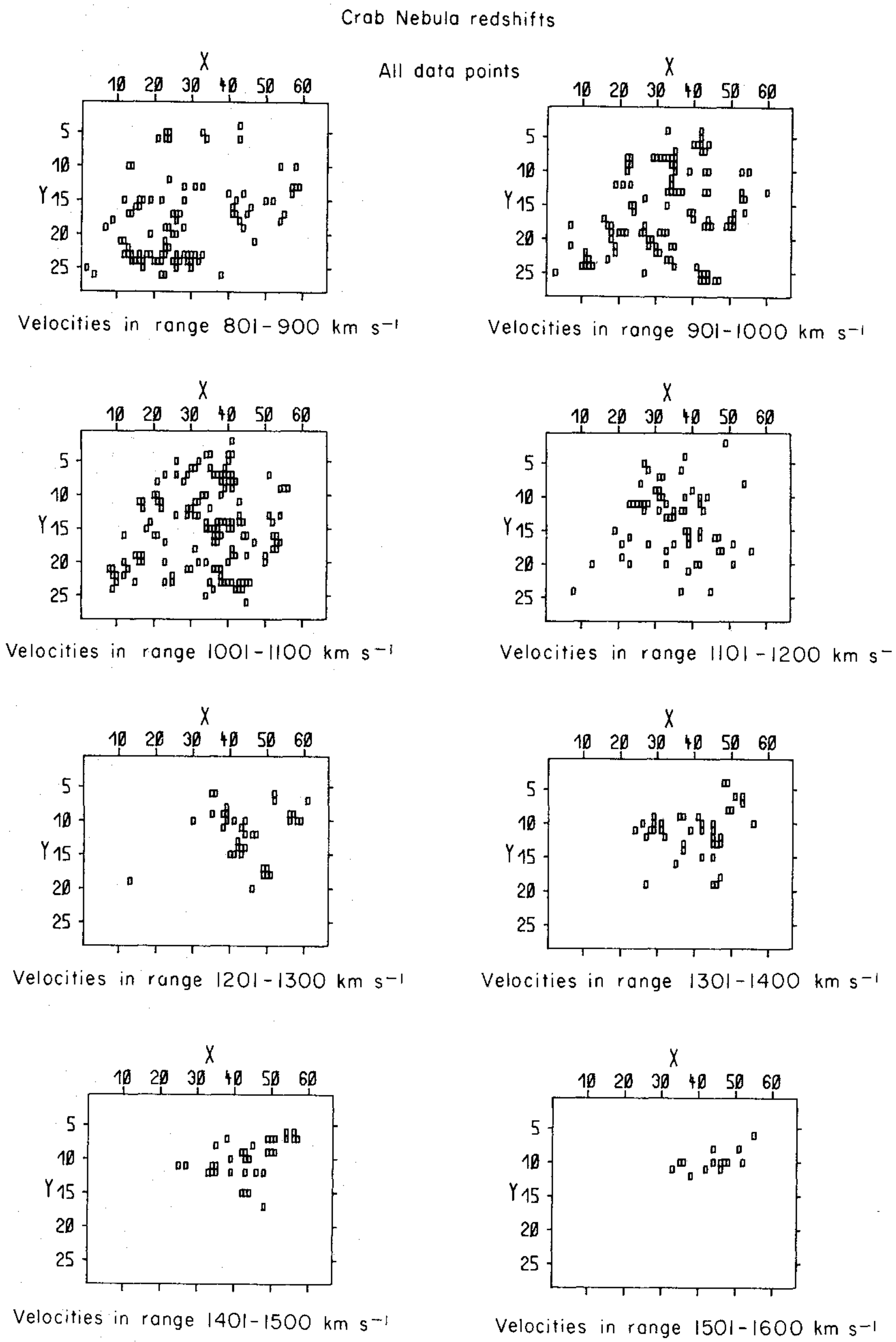

Figure 2 – *continued*

with Trimble's (1968) proper motion data, and again assuming a linear relationship between velocity and line-of-sight depth, the scale of the ordinate, in parsecs, is known. The scale of the abscissa depends on distance and this cannot be determined from the kinematic data alone. However, Trimble pointed out that for an expanding shell it is possible to make some estimate of distance by supposing that the maximum line-of-sight velocities should be the same as those in the plane of the sky. In fact she made comparisons between these velocities and the maximum proper motions at the extrema of the major and minor axes of the nebula

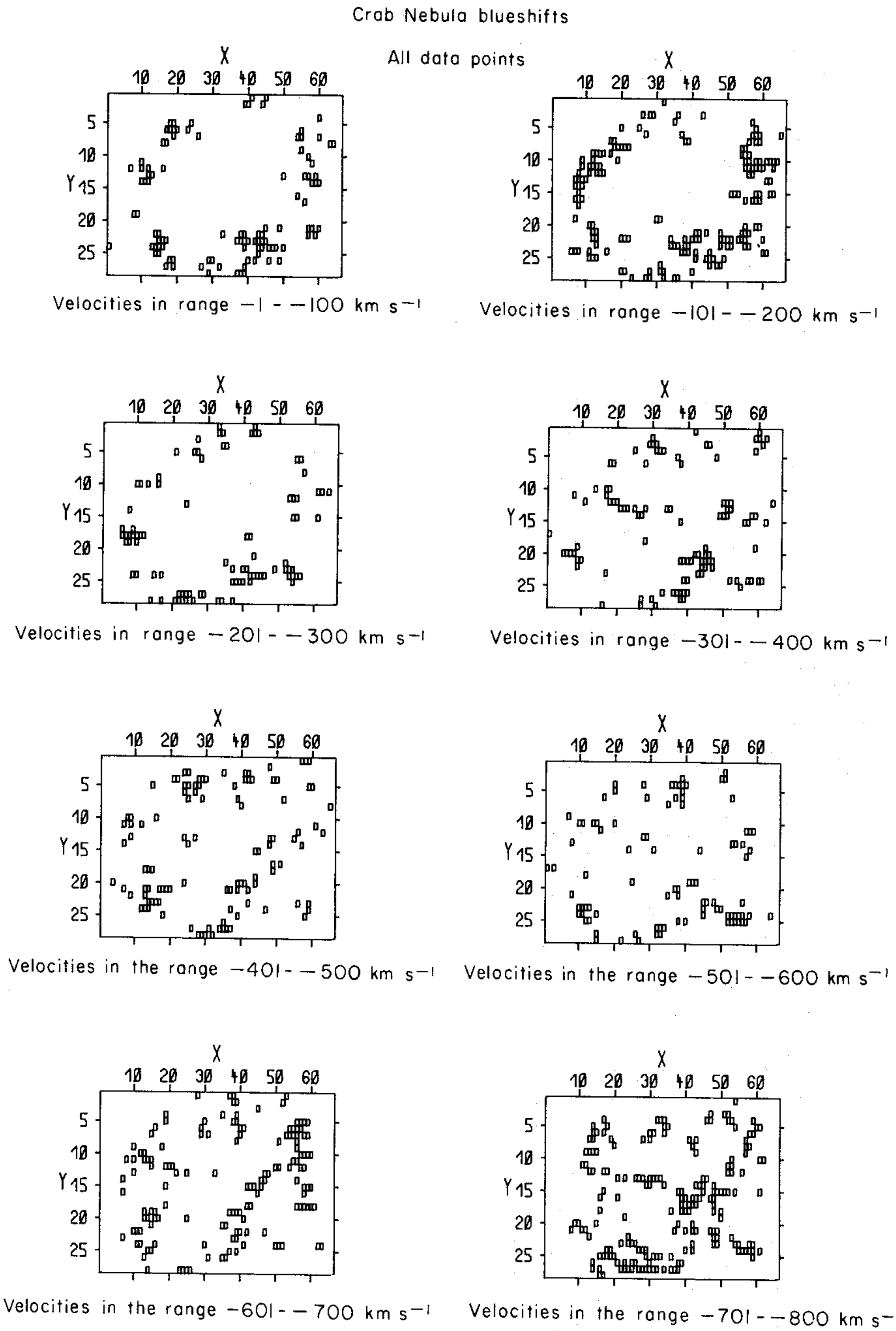

Figure 3. As Fig. 2, but blueshifts.

and found distances of 1.38 and 2.02 kpc respectively. Fig. 8 shows a pair of sections for the smaller distance and another for the larger, one merely being a horizontal rescaling of the other. These diagrams show at once that making velocity comparisons in this way is equivalent to assuming an overall shape for the outer envelope of the expanding shell, an oblate or a prolate spheroid, respectively.

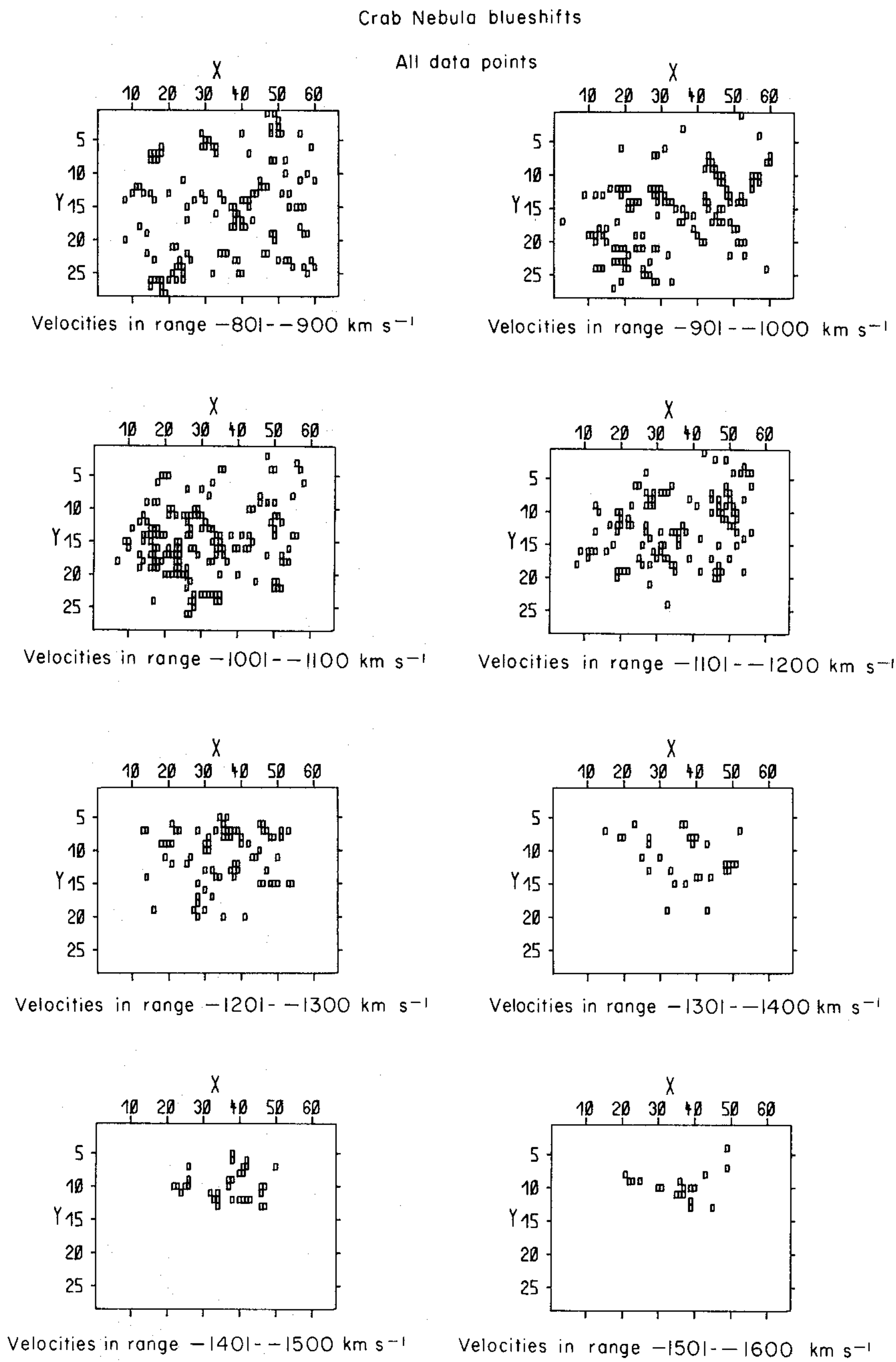

Figure 3 – *continued*

3.3 NARROW-BAND PHOTOGRAPHY

Combinations of the velocity sections of Figs 2 and 3 can be superimposed to simulate narrow-band interference photographs of the Crab Nebula. Chevalier & Gull's (1975) picture was intended to be a section through the centre of the Nebula at 5007 Å and shows

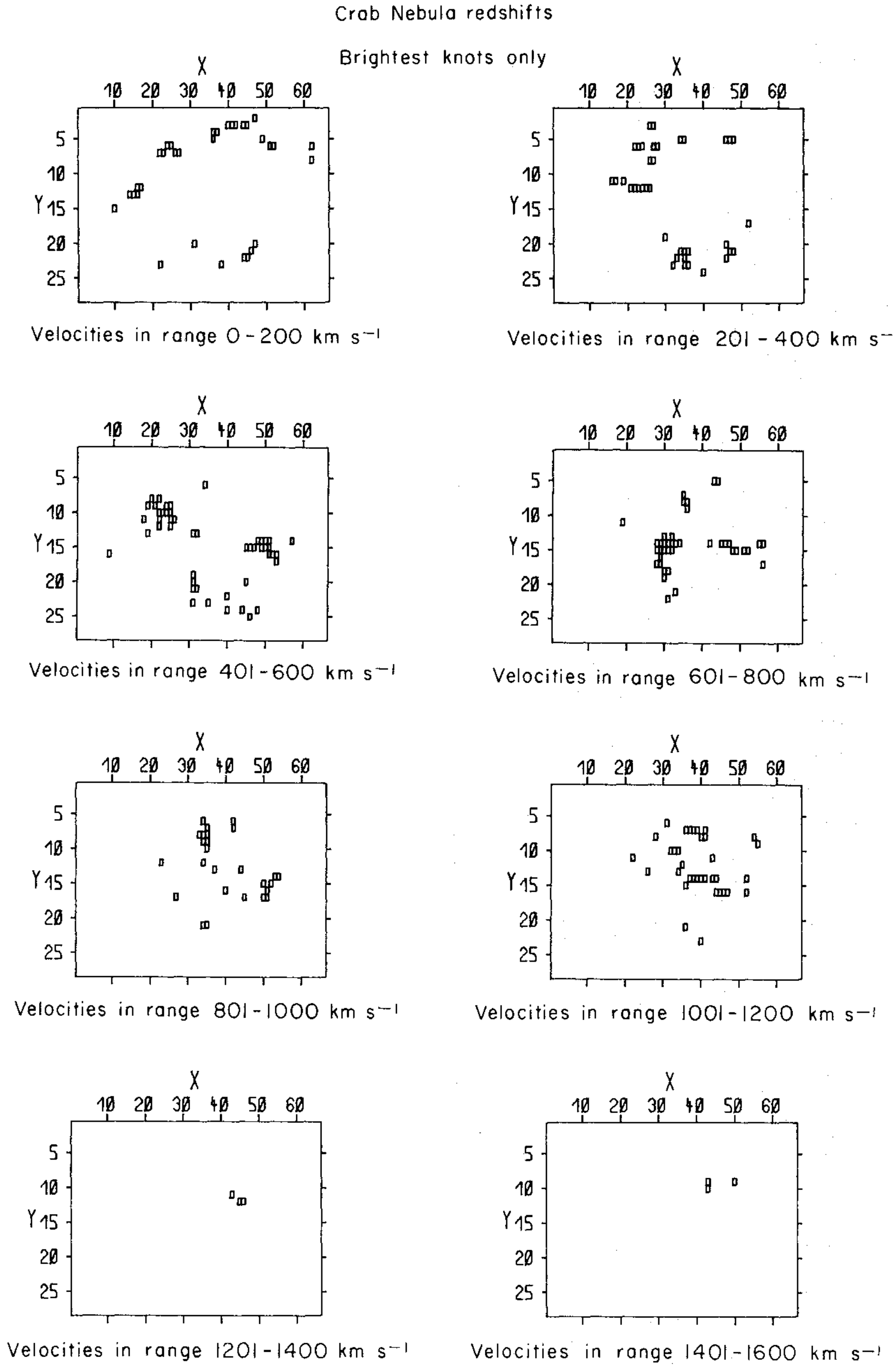

Figure 4. As Fig. 2, but brightest filaments only (200 km s^{-1} sampling).

knotty filaments within the shell. However, its appearance can be closely simulated by combining from Figs 2 and 3 pictures of blueshifted material between 200 and 1000 km s^{-1} (equivalent filter response centred at 4997 Å, 7 Å bandpass) and the knots are evidently near-side material. Wyckoff *et al.*'s (1976) picture of the far side of the Crab Nebula (nominally 5028 Å, 36 Å bandpass) actually includes bright blue-shifted material at -400 km s^{-1} which has crept into the picture in the wings of the interference filter (equivalent filter response centred at 5017 Å, 30 Å bandpass).

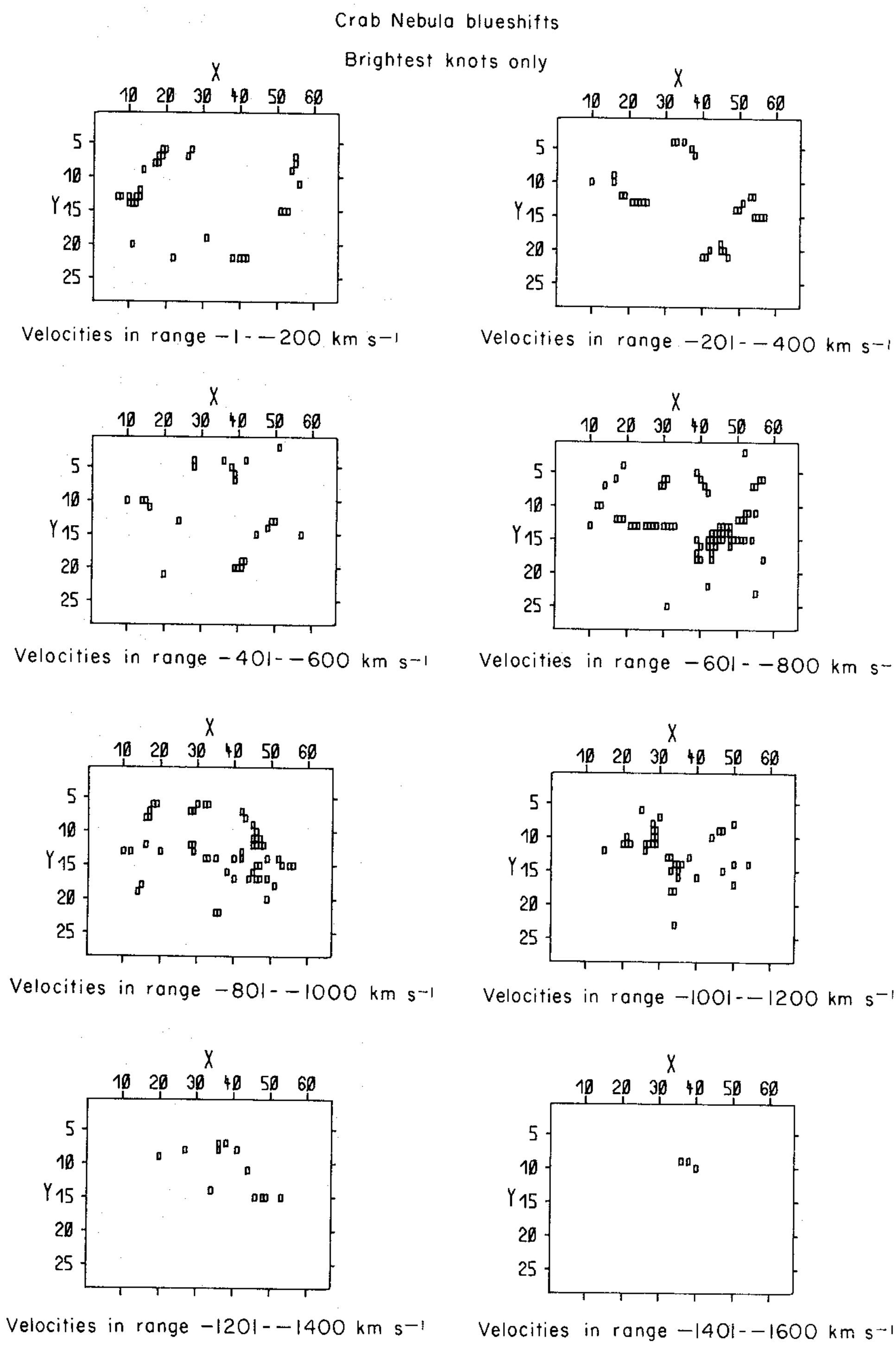

Figure 5. As Fig. 4, but blueshifts.

3.4 STRUCTURE WITHIN THE THICK SHELL

Fig. 1(a) shows that there is considerable structure within the thick shell. The brightest emission is concentrated to an inner velocity ellipse at $V_r \sim 1000\,\mathrm{km\,s^{-1}}$, beyond which lies a fainter emission complex, or second shell, at $V_r \sim 1500\,\mathrm{km\,s^{-1}}$. Isolated fragments of emission lie in a halo outside this second shell. The largest velocities lie not, as might be expected, at the centre of the nebula, but are concentrated to the north-western sector. This can be seen (a) by reference to Plate 1, where the deepest red and deepest blue points show

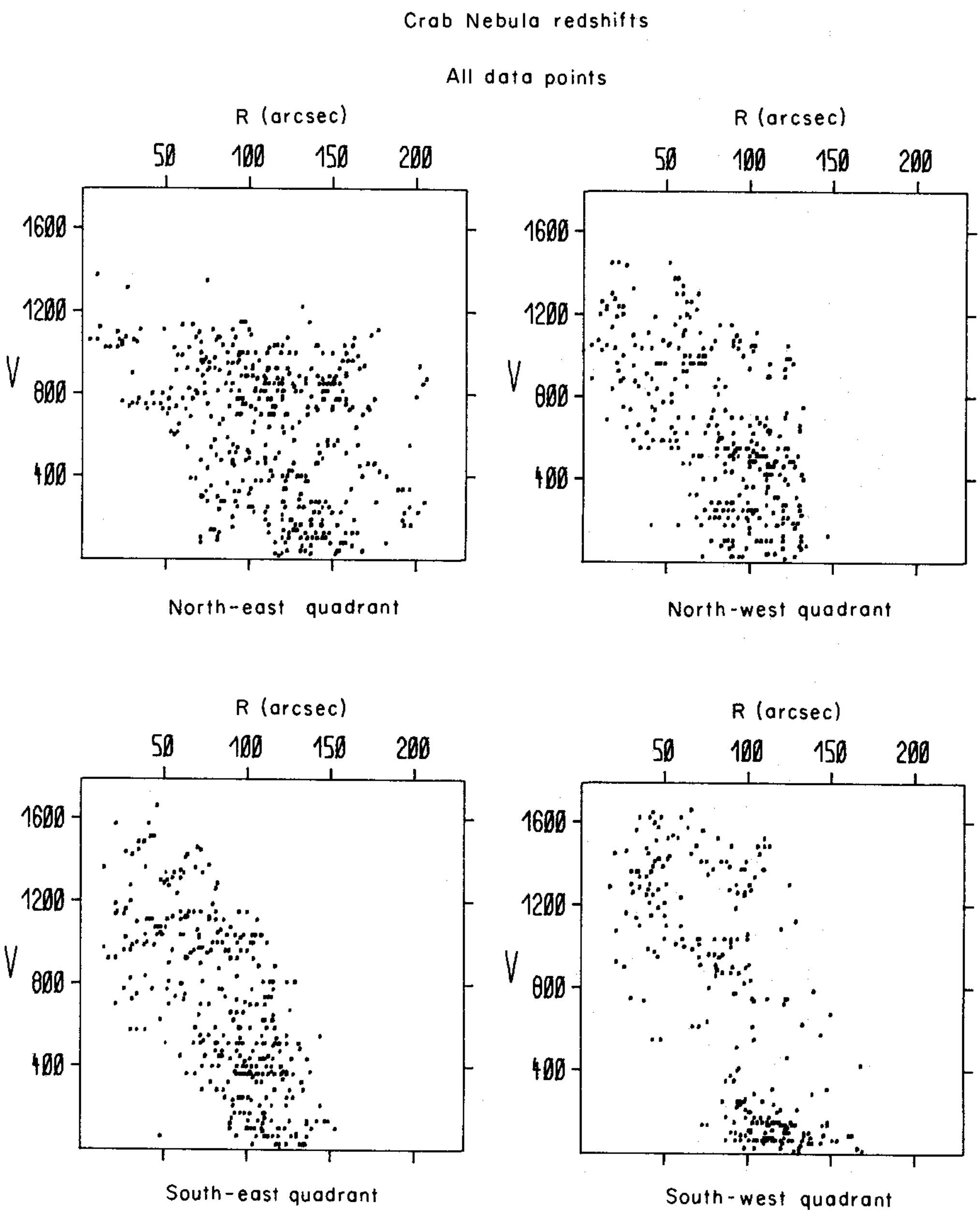

Figure 6. For each quadrant of the Crab Nebula the redshifted velocities at each point have been plotted against their radial distance from the pulsar. Note the thickness of the expanding shell and the hollow centre.

in the upper right-hand half of the nebula and (b) by reference to Figs 2 and 3, where the points with $|V_r| > 1401 \mathrm{~km~s^{-1}}$ cluster near $X = 40$, $Y = 10$, significantly north-west of the pulsar. Since the maximum redshift and blueshift both occur on the same north-west side of the Crab, this effect cannot be a consequence of a tilted geometry. It appears to be a manifestation of the outer velocity halo which is strongest in a cap fitted over the north-west end of the elliptical projection of the nebula.

Mayall (1962), Trimble (1968) and Chevalier & Gull (1975) have suggested that the filaments in the Crab Nebula run somewhat radially from the centre. The sections in Figs 2 and 3 which cut the nebula at ± 701–$800 \mathrm{~km~s^{-1}}$ lie within the thickness of the shell, and show that filaments approximately 10 pixels (~ 1 pc) long, but unresolved in width or

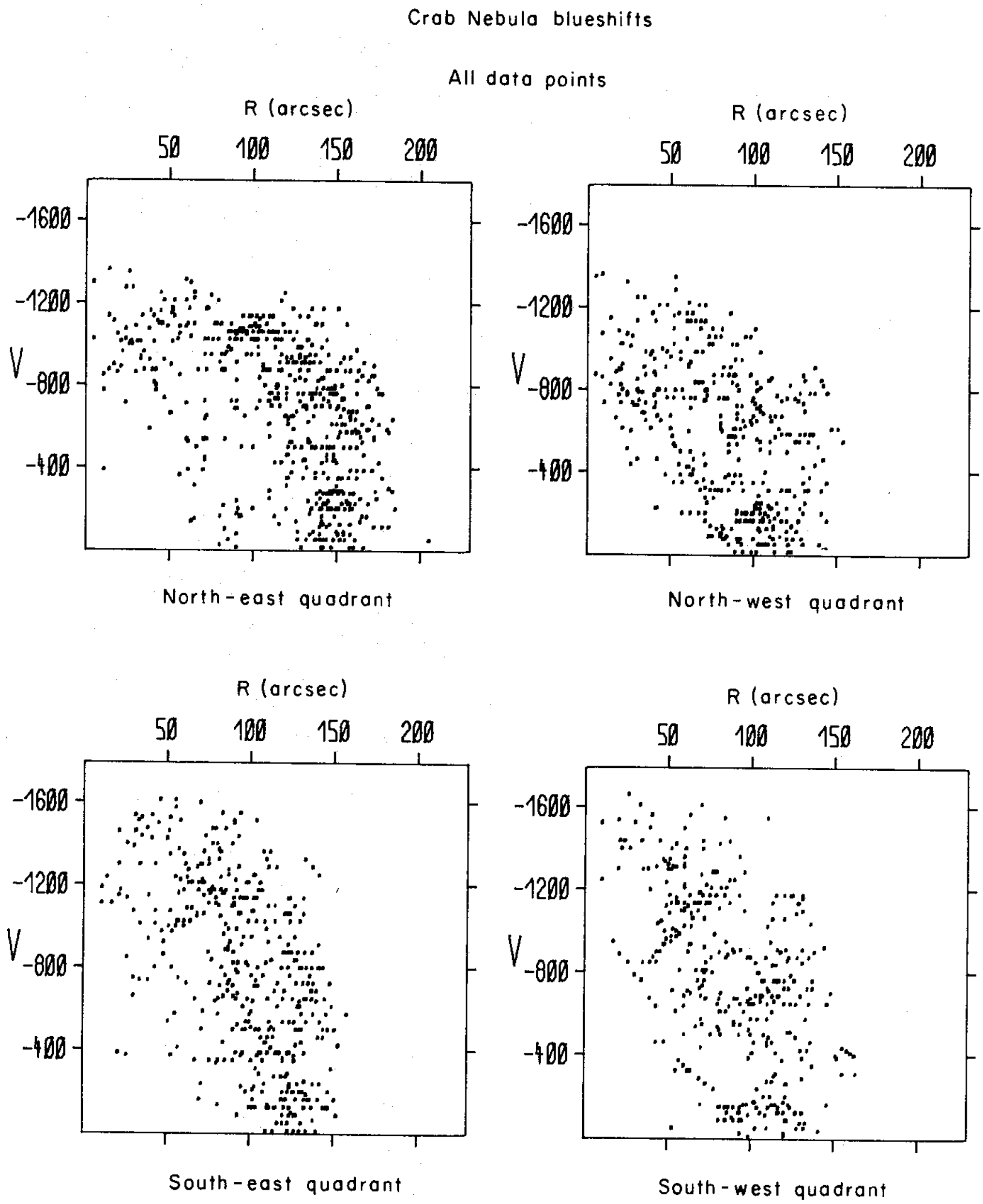

Figure 7. As Fig. 6, but blueshifts.

depth by this sampling (0.1 pc thick), lie in fact approximately circumferentially to the shell. Filaments are, however, angled across the thickness of the shell: for instance in Fig. 2, a filament runs from $X = 10$, $Y = 10$, $V_r = 150\,\mathrm{km\,s^{-1}}$ to $X = 25$, $Y = 12$, $V_r = 250\,\mathrm{km\,s^{-1}}$. A near-radial filament linking the two shells is visible in Fig. 1(a) at near-zero radial velocity, being at channel 380 in the easternmost (bottom) spectrum and running west for 17 spectra. A similar filament links the two shells at the west. (The 'coincidence' that there exist near-radial filaments at the east and west extremities of the Crab is because they are easiest to see at the extremities of Fig. 1a. Filaments can be traced across the two shells, with more difficulty, elsewhere.)

The filaments have been likened to a net (e.g. Minkowski 1966); we could extend the analogy and say that they were like a tangled net, loosely bundled around a hollow ball.

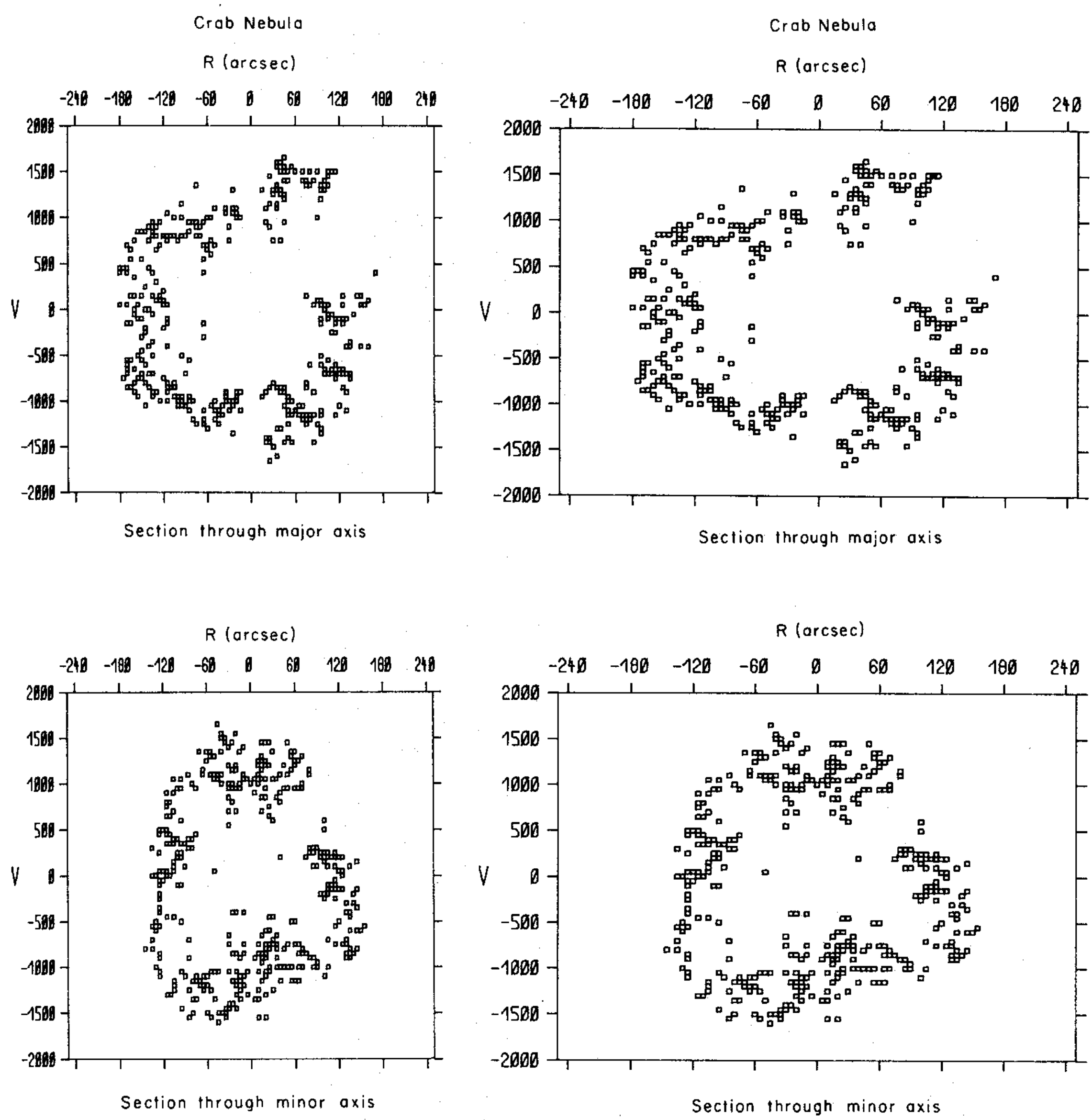

Figure 8. Cross-sections through the major and minor axes of the projected image of the Crab Nebula for different assumed distances. The diagrams have been scaled so that, for each vertical pair, linear distances are the same in each coordinate. The left pair of diagrams has been constructed for $d = 1.38$ kpc, the right pair for $d = 2.02$ kpc.

3.5 SURFACE BRIGHTNESS DISTRIBUTION

If the Crab Nebula is made up of a shell of well-separated thin filaments of uniform luminosity, then the filamentary system will show no central brightening. The facts contradict this supposition: the reality is that the brighter filaments occupy the central region of the nebula about 3.5 arcmin in diameter.

Possible explanations are:

(a) Filaments are not well-separated, but overlap. (But in a hollow shell model, this produces limb brightening, not central brightening).

(b) Filaments are not rope-like but ribbon-like, with flat surface across their radius vector from the centre.

(c) Filaments are not of uniform brightness.

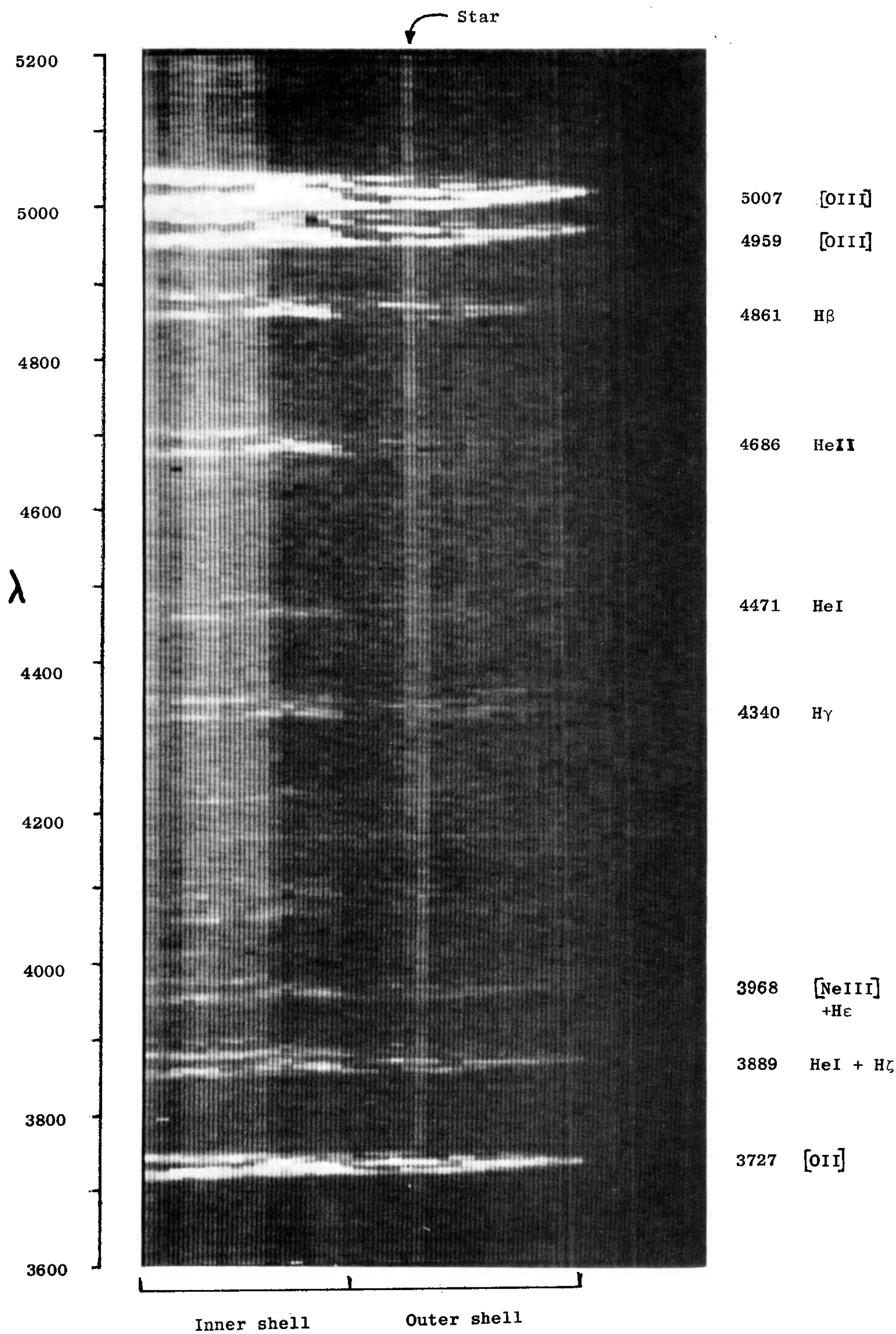

Plate 2. A photographic representation of an IPCS spectrum obtained with a 3 arcmin long slit oriented east–west and extending out beyond the nebula from a point about 30 arcsec east of the pulsar. Each spectral line may be imagined as a perspective view of an east–west cross-section through the Crab Nebula. The inner and outer shells are joined by a near-radial filament and enclose the synchrotron continuum. The outer shell is faint in the spectral lines of helium: compare, for example, the λ4686 line of He II with the Hβ line which has nearly equal intensity in the inner shell.

[*facing page* 428]

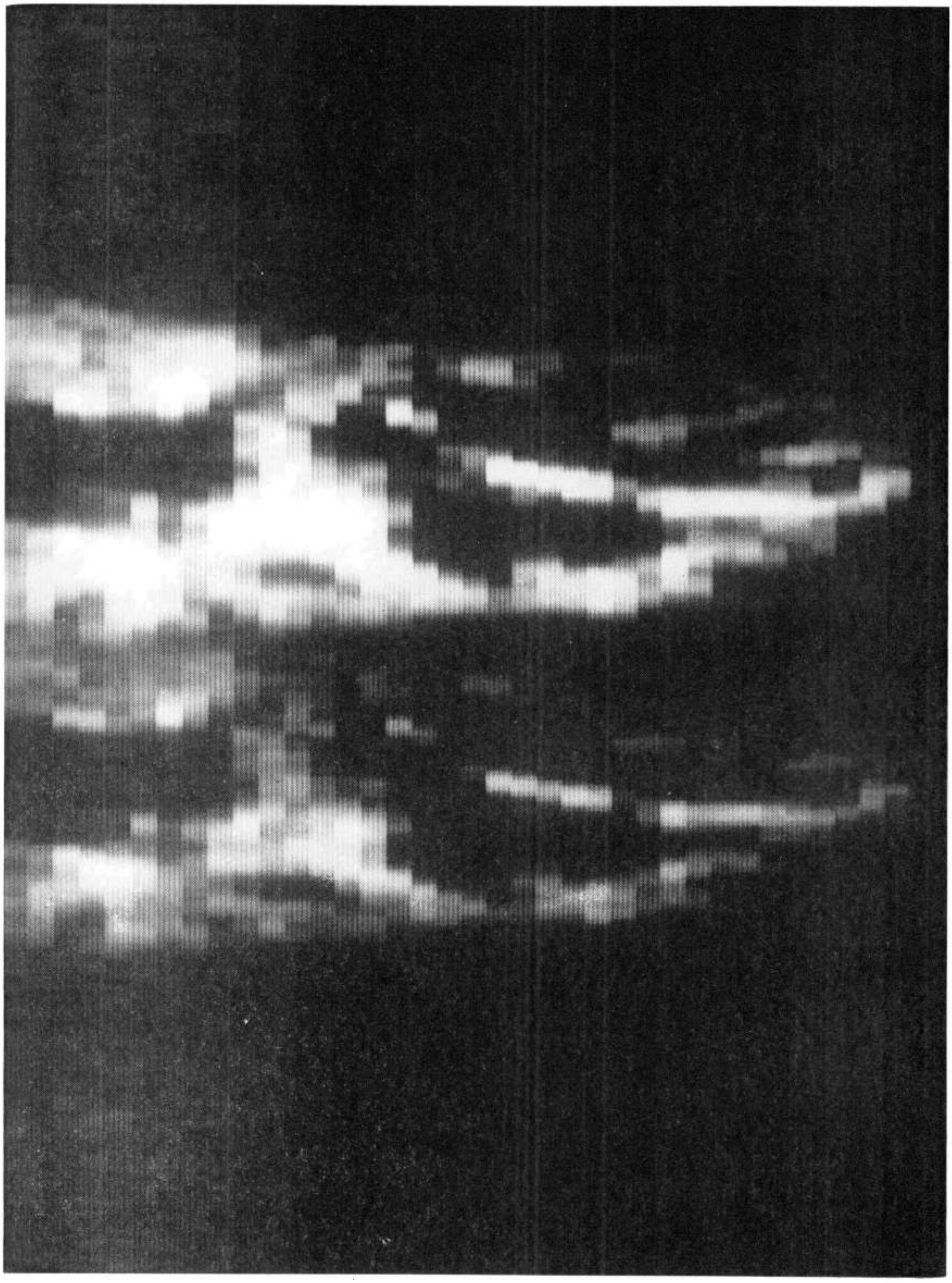

Plate 3. Enlargement of λ4959–5007 region of Plate 2 to show the detailed structure.

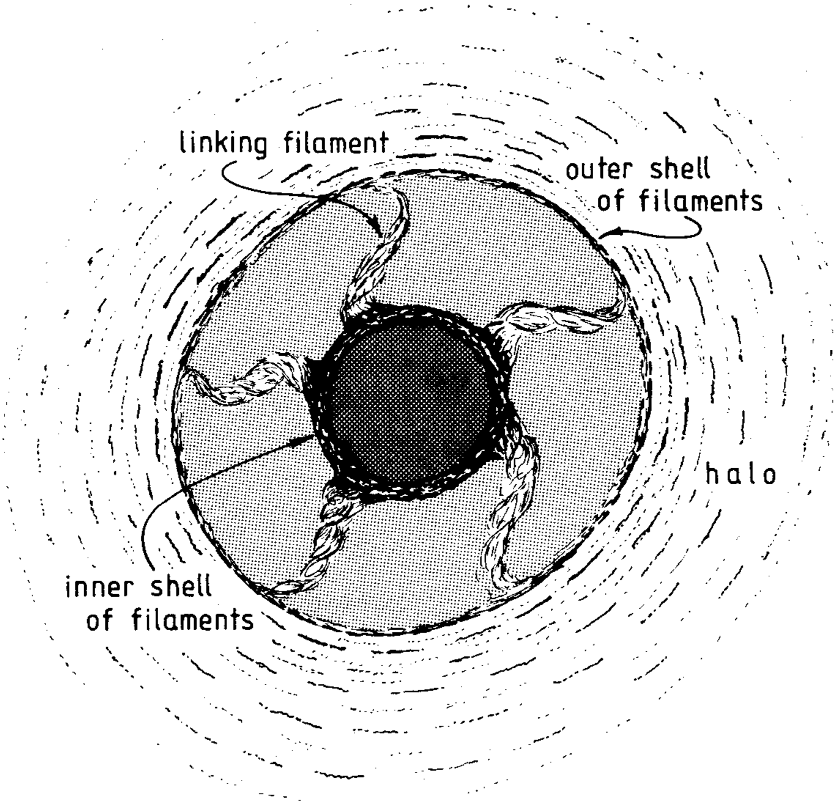

Figure 9. An idealized diagram showing a cross-section through the Crab Nebula. The dotted areas represent regions of synchrotron emission, high within the inner shell and weaker between the shells.

Fig. 1(a) shows that (c) is the likely explanation. The brighter filaments lie within the fainter, both at the centre of the nebula, where the $|V_r|$ of the brighter filaments is smaller than the fainter filaments, and at its periphery, where the fainter filaments extend beyond the brighter ones. Why are the filaments on the inner shell brighter? Possible explanations are:

(a) Filaments are illuminated and excited from the synchrotron radiation within the shell; the further filaments suffer a dilution effect. (But this seems an unlikely explanation. If the synchrotron radiation is highly centrally condensed, and the outer shell is ~ 1.25 times more distant from the centre than the inner, then the outer shell receives ~ 0.6 times as much radiation as the inner. If the synchrotron radiation is uniformly distributed within the outer shell, the dilution is less. This small dilution factor, of between 0.6 and 1.0, seems unlikely to account for an overall difference in intensity ~ 10 between the inner and outer filaments.)

(b) The inner filaments are different from the outer filaments in a way which makes them brighter. They may be denser, or thicker, or have a larger electron density or other composition-dependent difference, or may be exhibiting a boundary-layer difference.

3.6 SPECTRAL DIFFERENCE BETWEEN THE SHELLS

Plate 2 shows a photographic representation of the eastern half of a longer exposure (2 hr) spectrum (λλ 3727–5007) obtained with the IPCS on the AAT in 1982 January. Each spectral line may be imagined as a perspective cross-section through the Crab Nebula shells. The double-shell structure may be seen at the λλ 4959–5007 [O III] lines, λ 3727 [O II] and in Balmer emission. It is shown more clearly on Plate 3 where the λλ 4959–5007 section of

Plate 2 has been enlarged. Also clear is the near-radial filament linking inner and outer shell to the eastern side of the nebula.

Plate 2 brings out structural differences in the Crab Nebula as seen in different spectral lines. The most startling is that the outer shell is not seen in the spectal lines of helium. Although, for instance, the λ 4686 line of He II is as intense as the $H\beta$ line on the inner shell, it is very faint on the outer shell, and although λ 4471 of He I is almost as intense as $H\gamma$ on the inner shell it is much weaker on the outer shell. Spectral differences amongst Crab Nebula filaments have already been remarked upon. There are thus spectral differences between the shells. We note the 'remarkable spectra on the outskirts of the Crab Nebula' observed by Davidson (1978) who contrasts the spectra of the bright filaments normally observed (on the inner shell) with his spectra of fainter nebulosity (on the outer?). Henry & MacAlpine (1982) conclude that there are differences in relative helium abundance amongst the Crab Nebula's filaments. Plate 2 demonstrates correlation of these abundance variations with three-dimensional structure of the nebula.

Spectral differences between inner and outer shells might be explained in terms of the Type II supernova model proposed by Chevalier (1977). The inner shell now observed could have had its origin as helium-rich, outer core material of the progenitor not quite reaching nuclear densities during the core collapse producing the supernova event, and subsequently deriving its kinetic energy almost entirely from the pulsar: the high-velocity outer shell and halo would then be the shock ejected envelope of the progenitor.

3.7 THE SHELLS AND SYNCHROTRON EMISSION

At the declination of the pulsar, Fig. 1(a) shows that the brighter, inner shell extends 1.5 arcmin east and 1.9 arcmin west of the pulsar. Comparison with the radio synchrotron maps at 2.7 and 5 GHz (Wilson 1972) and optical continuum isophotes (Woltjer 1957) shows that the bright filaments correlate with a brighter central core to the synchrotron emission. The fainter synchrotron emission extends over a total of 5.4 arcmin, just to the boundary of the faint outer filamentary shell. The bright central regions standing on a plateau may also be seen in cross-sections through the optical continuum (Woltjer 1957).

Thus we can picture the relativistic electrons which produce the synchrotron emission to be, in the main, confined within the inner shell and to produce the bright region. However, electrons leak out through holes in the net of the inner shell and occupy the region between the filamentary shells. This produces the plateau of fainter synchrotron emission. This is confirmed in Plate 2. The bright synchrotron continuum comes to a near stop inside the inner shell of filamentary emission, but continues weakly through the outer shell. The same effect may be seen on a spectrum of the western half of the nebula.

4 Conclusion

The three-dimensional structure of the Crab Nebula is summarized as Fig. 9.

Acknowledgments

We wish to thank Stephen Richard who extracted the bulk of the radial velocities from the raw data, Michael Burton who completed the task, Elizabeth Swinbank who pointed out an error in our positional determination and Ken Hartley who produced the colourgraphs using the FR80 facilities at the Rutherford Appleton Laboratory. Plates 2 and 3 were produced at the RGO node of STARLINK using ASPIC software.

References

Chevalier, R. A., 1977. In *Supernovae,* p. 53, ed. Schramm, D. N., Reidel, Dordrecht, Holland.
Chevalier, R. A. & Gull, T. R., 1975. *Astrophys. J.,* **200,** 399.
Davidson, K., 1978. *Astrophys. J.,* **220,** 177.
Dennefeld, M., 1983. In *Supernova Remnants and their X-ray Emission, Proc. of IAU Symp. 101,* ed. Gorenstein, P. & Danziger, I. J., Reidel, Dordrecht, Holland (in press).
Deutsch, A. N. & Lavdovsky, V. V., 1940. *Pulkovo Obs. Circ.,* **30,** 21.
Duncan, J. C., 1939. *Astrophys. J.,* **89,** 482.
Henry, R. B. C. & MacAlpine, G. M., 1982. *Astrophys. J.,* **258,** 11.
Mayall, N. U., 1962. *Science,* **137,** 91.
Minkowski, R., 1966. In *Nebulae and Interstellar Matter,* p. 623, eds Middlehurst, B. M. & Aller, L. H., Chicago University Press, Chicago.
Münch, G., 1958. *Rev. Mod. Phys.,* **30,** 1042.
Murdin, P. G. & Clark, D. H., 1981. *Nature,* **294,** 543.
Swinbank, E., 1980. *Mon. Not. R. astr. Soc.,* **193,** 451.
Trimble, V., 1968. *Astr. J.,* **73,** 535.
Wilson, A. S., 1972. *Mon. Not. R. astr. Soc.,* **157,** 229.
Woltjer, L., 1957. *Bull. astr. Inst. Netherlands,* **13,** 301.
Woltjer, L., 1958. *Bull. astr. Inst. Netherlands,* **14,** 39.
Wyckoff, S. & Murray, C. A., 1977. *Mon. Not. R. astr. Soc.,* **180,** 717.
Wyckoff, S., Wehinger, P. A., Fosbury, R. A. E. & McMullan, D., 1976. *Astrophys. J.,* **206,** 254.

Monthly Notices
of the
ROYAL
ASTRONOMICAL SOCIETY

VOL. 204, NO. 1, 1983

David H. Clark, Paul Murdin, Roger Wood, Roberto Gilmozzi,
John Danziger and Andrew Furr

Three-dimensional structure of the Crab Nebula

Published for
the Royal Astronomical Society
by
Blackwell Scientific Publications Ltd
Osney Mead
Oxford
OX2 0EL

The microfiches are 105 × 148mm archivally permanent silver halide film
produced to internationally accepted standards in the NMA 98-image format

Microfiches produced by Micromedia, Bicester, Oxon

TABLE 1

Velocities in the Crab Nebula (Redshifts in km/sec)

COLUMN NUMBER X

ROW NUMBER Y	1	2	3	4	5	6	7	8	9	10	11
1											
2											
3											
4											
5											
6											
7											
8											
9											
10									142	142	

TABLE 1 (contd)

Velocities in the Crab Nebula (Redshifts in km/sec)

COLUMN NUMBER X

ROW NUMBER Y	12	13	14	15	16	17	18	19	20	21	22
1											
2											
3										105.	120.
4											254.
5							292.		67.	30. 254. 516.	30. 516.
6					30.	516.	441.		479.	67. 441. 628. 814.	67. 367* 740.
7							367.	591.	740.	441. 628.	67* 404. 702.
8		67.	30.					404. 591.	441*	479. 1000.	404* 963.
9	142. 441.			105.	67. 516.	628.	67. 516. 740.	516* 702.	591.	516*	516. 926.
10		814.	254. 814.	105. 479.	217. 404. 740.	441. 702.	367.	441. 702.	404. 665. 1037.	67. 404. 1000.	516* 963.

TABLE 1 (contd)

Velocities in the Crab Nebula (Redshifts in km/sec)

COLUMN NUMBER X

ROW NUMBER Y	23	24	25	26	27	28	29	30	31	32	33
1											
2									671.	553.	
3				135. 285*	210* 376*	376.	510.	540.	495. 645. 780.		
4			404.	367.	376.	450.	510.				930.
5	516. 889.	814.	180. 628.	329. 553. 1037.	330. 510. 1109.	345.	376.	421.	361.	450. 540. 1019.	480. 720. 840.
6	367* 814.	142* 367* 889.	30*	254.	255*	255* 1154.		1079.	1034*		450.
7	105* 367. 1037.	180.	254.	180* 1037.	105*		1064.		1183.	1124.	
8	367. 591. 963.		329.	292* 1112.	285*	1004*	944.	974.	974.	959.	944*
9	441. 926.	553*	404*	404.	450.		1367.	1152.	1124.		
10	479*	479*	553*	397. 1335.			1333.	1243.	1124. 1318.	1109*	1034*

1983MNRAS.204..415C

TABLE 1 (contd)

Velocities in the Crab Nebula (Redshifts in km/sec)

COLUMN NUMBER X

ROW NUMBER Y	34	35	36	37	38	39	40	41	42	43	44
1	487.			79.		211.				0.	40.
2	342.			105.	0.			1090.		53.	79. 723.
3			150.	90.	120.	75.	45*	45*	75*	75.	135* 750.
4	240. 1004.	180. 1004.	105*	105*	1154.		1064.	1034.	195. 915.	195. 840.	615. 750.
5	376*	240*	150*	120.	105.		1019.		900.	780*	780*
6	450* 780. 870*	1049. 1288.	1258.	1154.		1034.	959.	915.	900*	885.	944.
7	525.	510. 705* 900*	645. 1019*	1034*	1064* 1467.	1034*	1034.	1034*	944*	915.	
8	930*	750* 930* 1407.	720*	795.	795. 1034.	1243.	1094* 1630.	1034*	1004.		1571.
9	959*	900* 1273.	780* 1303.	1333.	1288.	1034. 1213.	1154.	1094. 1300.	1422.	1437*	
10	1034* 1660.	989* 1511.	1511.		1004. 1109.	989. 1273. 1452.		1213.	1154. 1362.	974. 1407* 1601.	944. 1183. 1273. 1422. 1571.

TABLE 1 (contd)

Velocities in the Crab Nebula (Redshifts in km/sec)

COLUMN NUMBER X

ROW NUMBER Y	45	46	47	48	49	50	51	52	53	54	55
1	60.	92.		105.	79.	789.		579.	92.	145. 316.	
2	119. 749.	119. 461. 749.	145*	132.	1129.		631.		53.	53. 290.	
3	79*	79. 316.	237.	198.	132.				13.	26.	
4	292. 553.			254. 1372.	1372.	142.	67.	67.	30.	105.	67.
5	254. 404. 516.	254*	254*	217*	105*	67.	67.	67.	67.		
6	254.	180.			67.		30* 1372.	67* 1298.	30. 1335.	1446.	1520.
7					1409.	67. 1409.	105. 1000. 1483.	105. 1298.	67. 1372.	1409.	
8	1446. 1668.			142.	142. 1353.	1372.	1520.			1186*	
9					1483.	1409*	1409.			1037.	1037*
10	1393.	1524.	1538.	1524.				1564.	798. 957.	865.	957.

TABLE 1 (contd)

Velocities in the Crab Nebula (Redshifts in km/sec)

COLUMN NUMBER X

ROW NUMBER Y	56	57	58	59	60	61	62	63	64	65	66
1					92.	26.	13.				
2	53.		671.								
3				132.	132.	60.	60.		92.		421.
4	142.										
5											
6	1483.			142.	67.	30.	105*				
7	1483.	1483.			142.	105. 1298.	142.				
8		740.		67.	67.	67. 217.	105*				
9	1037. 1260.	1260.			96.						
10	1274. 1393.	228.	825. 1248.	109. 1274.	149.		109.				

TABLE 1 (contd)

Velocities in the Crab Nebula (Redshifts in km/sec)

COLUMN NUMBER X

ROW NUMBER Y	1	2	3	4	5	6	7	8	9	10	11
11							105.	142.	217. 553.		30.
12										376.	329.
13											
14											
15									105.	67*	67.
16							30. 777.	553.	516*		
17		270.							777.	740.	740.
18							963.		814.		
19							516. 889.	777.	740.		
20				780.	735.	450.	740.	777.			777.

1983MNRAS.204..415C

TABLE 1 (contd)

Velocities in the Crab Nebula (Redshifts in km/sec)

COLUMN NUMBER X

ROW NUMBER Y	12	13	14	15	16	17	18	19	20	21	22
11	67.	142.	404.	292.	254* 1000.	217* 1037.	404* 777.	367* 709*	367. 665.	665. 1075.	479* 1000*
12	367.	367.	105.	142.	180*	105* 1037.	142. 367.	180. 516. 963.	217. 628.	254* 740. 963.	292* 516* 1000.
13			30*	67*	105*			591*		777.	588.
14								702. 1000.			
15	834.				851.	814.	1000.	889. 1149.			814.
16	1000.			851.	851.				1075.	1000.	
17		851.	814.		926.					1112.	
18		142.				926.	777. 963.				
19		1223.		1075.	1000.	1037.	911.	777.	926.	926. 1149.	777. 963.
20	1037.	1148.			1000.	1037.	926.	851.			

TABLE 1 (contd)

Velocities in the Crab Nebula (Redshifts in km/sec)

COLUMN NUMBER X

ROW NUMBER Y	23	24	25	26	27	28	29	30	31	32	33
11	516. 1112.	553. 702. 1112. 1372.	553. 1149. 1446.	516* 1149.	1124. 1422.	1154. 1318.	1333.		60. 1079. 1303.	1079.	1109. 1571.
12	329* 963*	292* 814.	367* 591*	367*	450. 1109. 1347.		510. 1079.	1079.	1109.	1362.	1482.
13				1037*	735.	705. 810.	630. 1049.	780*	570* 840. 1034.	570* 750* 1004. 1094.	570. 825. 959. 1198.
14			777.		915.	780*	750*	795*	750*	750*	735*
15	926.	963.			615.	615* 825.	720* 795.	750*	720*	780*	750. 900.
16	1112.	963.					705*	750.			
17	1075.		889.	814.	825*	780* 1139.	735*	720.			
18				851.	795. 915.		720.	645*	600* 1019.		1109.
19	851.	851.		926.	915. 1347.	885.	795.	391* 690*	540* 930.	989.	989.
20	1000. 1149.		814.	851.		974.	944.	795.	105* 300. 480*	391. 1079.	1139.

TABLE 1 (contd)

Velocities in the Crab Nebula (Redshifts in km/sec)

COLUMN NUMBER X

ROW NUMBER Y	34	35	36	37	38	39	40	41	42	43	44
11	989. 1482.	1452.			1273.	1362.			1139. 1362. 1567.	1094* 1288*	735.
12	720. 989* 1422.	1019* 1168. 1437.		1154.	1183. 1571.	1452.				1168. 1467.	1258.
13	780. 959. 1139*	705. 930. 1139.	930.	974* 1362.					1288.	930. 1079.	900*
14	765* 1034.			1064* 1377.	1064*	1019*	885. 1049*	1079*	690* 1228.	1034* 1273.	885. 1004* 1243.
15	1079.	1094.	1019*	1019.	1124.	1198.	1019. 1258.	1049. 1243.	840. 1139. 1303. 1452.	1243. 1452.	645. 1437.
16		1318.	1049.	1064.	1019.	959. 1183.	930*	870.	750. 1198.		1049*
17		1109.	1049.	1064.		1103.	944.	870.	855.		915.
18								750. 1034.	690.	840. 959.	959.
19								1049.	1064.	645. 780.	630. 885.
20	1019.						1094.	1124.	1198.		

TABLE 1 (contd)

Velocities in the Crab Nebula (Redshifts in km/sec)

COLUMN NUMBER X

ROW NUMBER Y	45	46	47	48	49	50	51	52	53	54	55
11	1306. 1624.	1508.									
12	1335* 1624.	1248* 1479.	1248. 1393. 1652.	1422.							
13	756. 1306.	1364.	1335.	553.	553. 1624.		1017.		611. 988.	611. 1017.	640.
14	740*	665*	628*	591*	591*	591*	591*	1000*	963*	963*	665*
15	591* 1326.	553*	553*	740*	591* 777*	553* 814*	553* 702*	628* 851*			
16	1037*	814. 1112*	1186*				479* 926*	479* 1000*	516* 1000.	254. 628. 963.	740.
17	180. 889*		1075.	1446.	1298.	963* 1298.	329. 963* 1186.	329*	30. 404* 1037.	105. 1037.	889.
18	963.		1149. 1372.	1186.	926. 1260.	963. 1260.	963. 1298.	1000.	292. 1037.	292. 628. 814.	180. 479.
19	180. 1037. 1372.	1335.				1000.				292.	292.
20	516* 702.	217* 1223.	180* 516.		217.	254. 1075.	292. 1149.	292.	292.	217.	254.

1983MNRAS.204..415C

TABLE 1 (contd)

Velocities in the Crab Nebula (Redshifts in km/sec)

COLUMN NUMBER X

ROW NUMBER Y	56	57	58	59	60	61	62	63	64	65	66
11				175.	146.	175.	146.	146.			
12		349.	146. 349.	87. 233.	117.		58.	146.	146.		
13		872.	378. 872.	408. 872.	87. 262. 901.	175.	146.	175.		117.	
14	254. 665*	441* 851.	441.	329.	292.						
15											
16											
17	740*										
18	30. 702. 1149.	30.		367. 628.		367.					
19		67. 553.									
20	142. 516.	516. 702.	553.	628.							

Velocities in the Crab Nebula (Redshifts in km/sec)

COLUMN NUMBER X

ROW NUMBER Y	1	2	3	4	5	6	7	8	9	10	11
21							926.	1037.	1037.		851.
22									67. 1037.	1000.	926.
23		336.	339.							1075.	963.
24	270.	226.	166.	166. 226.				1112.	1083.	934.	993.
25		874.	934.								726.
26				845.	785.	250. 547.	190.	339.		71. 398.	428.
27											
28											

Velocities in the Crab Nebula (Redshifts in km/sec)

COLUMN NUMBER X

ROW NUMBER Y	12	13	14	15	16	17	18	19	20	21	22
21	851.	553. 1037.	30.				142.	926.			
22	1000.	814.						702. 926.	30. 217. 777.	30. 740.	777.
23	814. 963.	889.	889.	1000.	889.	926.	404. 851.	292. 665. 889.	142.	105.	105* 814.
24	963.	904.	845.	845.	845.	250. 874.	458. 726.	160. 785.	131. 874.	101. 815.	160. 815.
25	696.	636.	339.	131.	41.	547. 874.	131.				
26	458.	458.	41. 398.	131. 547.	131.	755.	220.		220. 726.	577.	190. 488. 815.
27							190.	726.	71. 270. 755.	220.	160. 577.
28											

TABLE 1 (contd)

Velocities in the Crab Nebula (Redshifts in km/sec)

COLUMN NUMBER X

ROW NUMBER Y	23	24	25	26	27	28	29	30	31	32	33
21	814.		777.	777.		944.	675. 1034.	645. 915. 1079.	135. 570*	135. 345. 540* 690.	270. 435. 750*
22	814.	814.	1000.	740.	750.	705.	705.	555. 944.	510. 735* 900.	361. 585.	270*
23	814. 1037.	740.	777. 1000.	887.		825.	615. 885.	525. 885.	480* 885.	376* 750.	330. 810. 989.
24	190.	250.	874.	874.	845.	428.	458. 874.	488. 815.	369. 696.	458. 879.	369. 726.
25		160.		190. 845.	131. 904.	339. 696.	398. 636. 785.	12. 517. 845.	71. 488.	696.	398. 696.
26	220. 845.	220.	190.	101. 696.	250.	41. 398.	398.	458. 577.	428. 636.	428.	41. 398.
27	220.	131. 250.	101. 274.	101.	279.	131. 279. 458.	101.	279.	369.	41. 369.	
28		71.	71.	41.		71.			130.	160.	160.

TABLE 1 (contd)

Velocities in the Crab Nebula (Redshifts in km/sec)

COLUMN NUMBER X

ROW NUMBER Y	34	35	36	37	38	39	40	41	42	43	44
21	330* 974*	300* 944*	75. 300* 1004*	1049.	1094.	1109.					
22	270. 480.	120. 240*	105. 300.	90.	495. 1064.	510.	555*		585.	600.	75* 600.
23	255. 540. 944.	270* 510. 1079.	330* 450.	195. 465.	150* 480. 1034.	30. 180. 495. 1049.	75. 525. 1079*	570. 1049.	540.	555. 1094.	511. 1034.
24	220. 666.	250. 607. 934.	339. 1083.	309. 517. 1112.	250. 488.	166. 488.	250* 488*	458. 666. 934.	1053.	488. 1023.	488* 1053.
25	131. 369. 636. 1023.	160. 696.	250.	190. 547.	220. 488.	279. 517.	101. 339.	101. 398. 696.	41. 458. 636. 904.	428. 636. 904.	458. 964.
26	71. 369. 696.	339.	279. 607.	279.	190. 845.	100.	250.	190.	398. 696. 934.	12. 547. 696. 904.	517. 726. 993.
27		309.	309.	250.	250.	71. 279.	666.	250. 636.	101. 220.	131. 428.	398. 755.
28	226.										

TABLE 1 (contd)

Velocities in the Crab Nebula (Redshifts in km/sec)

COLUMN NUMBER X

ROW NUMBER Y	45	46	47	48	49	50	51	52	53	54	55
21	665.	105* 702.	217* 404. 851.	217*	254.	105. 254.	105.	217.		254.	254.
22	105* 553.	217* 553.	67. 516.	30. 254. 628.		702.	217.	254. 591.		105.	
23	553. 1075.	30. 404. 1000.	67. 367.	195. 555.	240. 540.	105. 255. 525.	450. 675.	510.	480.	234.	180.
24	577. 1112.	517.	517.	428* 666.	41. 428.	428.	41. 309.	309. 547.	279.		
25	458.	488*	488.	428. 607.	130. 458.	279.					
26	369. 547. 1053.	488. 993.	190. 488. 964.	160. 458.	190. 517.						
27											
28											

TABLE 1 (contd)

Velocities in the Crab Nebula (Redshifts in km/sec)

COLUMN NUMBER X

ROW NUMBER Y	56	57	58	59	60	61	62	63	[illegible]	65	66
21	217.	180.	105.								
22	105.	180.	67.	217.	30.	67.					
23	210.				75.						
24	309.						131.				
25											
26											
27											
28											

TABLE 2

Velocities in the Crab Nebula (Blueshifts in km/sec)

COLUMN NUMBER X

ROW NUMBER Y	1	2	3	4	5	6	7	8	9	10	11
1											
2											
3											
4											
5											
6											
7											
8											
9							-570.			-649.	
10								-495.	-195. -495.	-232* -533*	-232. -570.

1983MNRAS.204..415C

TABLE 2 (contd)

Velocities in the Crab Nebula (Blueshifts in km/sec)

COLUMN NUMBER X

ROW NUMBER Y	12	13	14	15	16	17	18	19	20	21	22
1											
2											
3											
4						-796.		-683*	-533.	-495.	-495.
5			-721.	-495.			-7. -796.	-7. -608. -1022.	-195. -533. -1097.	-232. -1060.	
6			-796.	-721.	-645.	-45. -570. -796*	-82. -345. -834. -1097.	-45* -382. -909*	-45*	-1286.	
7		-796. -1248.	-796* -1286.	-645. -871. -1324.	-871.	-100. -871*	-120* -871.	-45* -721.			-1211.
8				-834.	-82. -871*	-82* -871*	-120*	-120. -1362.	-195. -758. -1362.	-120. -1513.	-120.
9	-157. -758.	-195. -721. -1135.	-157* -721.	-195. -796. -1060.	-270*	-120. -1022.	-645. -1097. -1286.	-1211.	-1248*	-1211.	-1551.
10	-157. -645*	-232. -608*	-382. -533* -1135.	-533*	-270* -495.	-382.	-382.	-157. -1135.	-533. -1135.	-1060*	-1097. -1400.

TABLE 2 (contd)

Velocities in the Crab Nebula (Blueshifts in km/sec)

COLUMN NUMBER X

ROW NUMBER Y	23	24	25	26	27	28	29	30	31	32	33
1						-634.				-185.	-251.
2								-370.			-290.
3		-437.	-422.	-196.	-226.	-156.	-196. -361.	-392.	-392.		
4			-345.		-1102.	-407* -512.	-437. -829.	-437.	-392.	-376* -708.	-316* -739.
5		-7. -458.	-120. -458.	-232.	-286. -497.	-497*		-648. -814.	-829.		
6	-7. -1324.	-458. -1173.	-1135*		-196* -497.	-226. -376.	-527. -678. -829.	-708* -829*	-739* -920.	-890*	-890* -1011.
7	-1248.		-495.	-82* -1060. -1437.	-1117.	-724. -905* -1269.	-437. -663. -966* -1162.	-708* -1056*	-633. -1117.	-1193.	-875. -1178. -1299.
8					-1360*	-1132*	-1162.		-1208.	-1056.	
9	-1135. -1513.		-1551.	-1475.	-1117. -1329.	-1147*	-1177*	-1208.	-1269.		
10	-1475.		-1475.	-1437.		-1087*	-1087*	-1223. -1511.	-1238. -1572.		

TABLE 2 (contd)

Velocities in the Crab Nebula (Blueshifts in km/sec)

COLUMN NUMBER X

ROW NUMBER Y	34	35	36	37	38	39	40	41	42	43	44
1				-608.	-634.			-79.	-383.	-290. -1169.	
2	-277.				-647.	-13. -647.	-26.		-264.	-264.	-92. -264.
3		-497.	-135. -920.			-572.		-452.	-482.	-196.	
4	-226. -708.	-120. -211* -633. -1072.	-512* -588. -1072.	-542.	-573.	-648.	-573. -875.	-497.	-407*	-467.	
5	-769. ·1284.	-784.	-1223.	-346*	-497* -663. -1496.	-557. -678*					
6	-799. -1162.	-1238.	-1375.	-135. -573. -1329.	-341* -1405.	-542*	-648*	-678.	-1420.		
7		-588. -1208.	-1223*	-1299.	-166. -1299* -1603.	-166. -437* -573* -1269. -1615.	-693.	-739* -1436.	-814* -1405.	-799. -920.	
8		-1208.	-1238*	-1299.	-1344.	-693. -1117. -1329.	-497. -1208. -1360. -1496.	-1405.	-708*	-935* -1557.	-935.
9	-1618.		-1527*	-1466.	-1420*	-1329.	-1299.	-1178.	-950. -1299.	-708. -1314.	-981.
10	-1618.			-1420. -1542.		-1557.	-1557*			-1041.	-1056*

TABLE 2 (contd)

Velocities in the Crab Nebula (Blueshifts in km/sec)

COLUMN NUMBER X

ROW NUMBER Y	45	46	47	48	49	50	51	52	53	54	55
1	-79.		-873.		-899.			-926.	-647.	-700.	
2		-1178.		-489. -1085.	-1135.	-846.	-581*	-647*			
3	-303. -661.	-317.	-766.	-899.		-515. -859.	-515. -793.	-766.		-1164.	
4		-796.	-758.	-871.	-458. -1022. -1551.	-458. -834. -1064.	-834. -1173.	-758.	-758. -1173.		-1173.
5				-382.						-758.	
6	-1211.	-1248.			-1173.				-570.	-683.	-45. -270. -645.
7	-1173.	-1286.	-1286.		-1173. -1551.	-1135. -1437.	-1248.	-495. -1362.	-608. -1286.	-7. -645*	-45* -683*
8	-1135.	-1097.	-1172.	-811. -1226.	-871. -1211.	-1173*	-608. -1211.	-886.		-120. -1173.	-157* -1097.
9	-984*	-1097*	-1173*	-1060.	-1135.	-1060.	-1135.			-120*	-82.
10	-958. -1119. -1240.	-972* -1401.	-998. -1159. -1427.	-1106.			-1186.	-851. -1132.	-798.		-144. -945.

TABLE 2 (contd)

Velocities in the Crab Nebula (Blueshifts in km/sec)

COLUMN NUMBER X

ROW NUMBER Y	56	57	58	59	60	61	62	63	64	65	66
1		-436.	-422.	-409.	-317.						
2				-383.	-317.		-396.				
3	-1032.					-396.					
4	-871. -1135.	-120. -909. -1097.		-345. -721.	-38.						
5	-645.	-645.	-120. -645.	-420. -683.	-420. -721.	-758.					
6	-270. -608* -1135.	-120. -683*	-120. -721. -1060.	-157. -721. -871.						-157.	
7	-120. -683.	-721.	-157. -683.	-120. -683.	-82. -909.						
8	-677.	-232. -796.	-758.	-947.	-909.			-45.	-45.	-458.	
9	-120. -645.	-721.									
10	-104. -918.	-91. -651. -918.	-157. -664. -878.	-170. -651.	-664.	-144. -717.	-157. -758.	-170.	-144.		

TABLE 2 (contd)

Velocities in the Crab Nebula (Blueshifts in km/sec)

COLUMN NUMBER X

ROW NUMBER Y	1	2	3	4	5	6	7	8	9	10	11
11							-420.	-307. -608.	-120. -458.	-7. -683.	-157. -721.
12							-82.	-120.		-68.	-120. -382. -871.
13							-157*	-120* -570.	-157. -458. -909.	-120* -645* -871*	-1060.
14							-195. -420. -683.	-270. -871.	-120.	-82*	-45*
15								-195.	-1097.	-1097.	
16							-120. -645.		-120. -1173.	-1097.	-1135.
17	-301. -573.		-542. -905.			-226.		-157.	-270.		-1173.
18						-271.	-232. -1097.	-270. -1173.	-270.	-270.	-270.
19							-120. -270.	-82. -270.	-82. -307.	-232. -947.	-984.
20				-422.	-392.	-392.	-345.	-382. -871.	-798.	-785.	-195*

TABLE 2 (contd)

Velocities in the Crab Nebula (Blueshifts in km/sec)

COLUMN NUMBER X

ROW NUMBER Y	12	13	14	15	16	17	18	19	20	21	22
11	-195. -495. -796.	-195. -645.	-157. -683. -1060.	-608.	-533*	-345.		-1211.	-1135*	-1097*	-1173*
12	-82. -834.	-120* -758. -1022.	-157. -796.	-120. -683. -1022*	-7. -984*	-796* -1173.	-345* -758* -947.	-382* -608* -947. -1135.	-382. -645. -984. -1173.	-683. -984. -1248.	-1173.
13	-7* -947*	-7* -871. -1135.	-947.	-834.	-1022.	-1022.	-1022.	-909. -1135.	-871*	-345* -758*	-345* -645*
14	-82*		-1022. -1211.	-1022.	-871.	-1022.	-1022.	-1060.	-1022.	-984.	-909.
15			-1097.		-1060.	-721.	-1135.	-645.		-984.	-947.
16	-1135.	-1172.			-721. -1135.	-1060.	-1097.			-721. -1060.	
17		-1060.			-1060.	-1022.	-984.		-1060.	-1022.	-1060.
18	-232. -533. -871.	-495. -984.	-420. -1022.	-458. -909*	-796.	-1060.	-1060.	-683. -1022.			
19	-909.	-683. -1022.	-834* -984.	-645.	-645. -1060. -1248.	-1022.	-1060.	-1135.	-1135.	-1135.	-1135.
20	-195. -909.	-645.	-683.	-721. -947.	-645.	-645.		-1135.	-1097.	-1060.	-1060.

1983MNRAS.204..415C

TABLE 2 (contd)

Velocities in the Crab Nebula (Blueshifts in km/sec)

COLUMN NUMBER X

ROW NUMBER Y	23	24	25	26	27	28	29	30	31	32	33
11	-1097	-834 -1400	-1060 -1362	-1060* -1286	-1026*	-1026*	-1026*	-1072 -1344		-1496	
12	-1173		-1211	-1022*	-996 -1172	-573 -996*	-542 -996*	-981	-1072		-1436
13	-345* -721*	-232* -495*	-345* -645*	-721*	-407 -754* -1026 -1162 -1375	-376 -799* -981	-860* -920	-799* -1011 -1299	-739* -935 -1147	-739* -1011* -1299	-663 -754* -1072* -1390
14	-947	-533 -947	-495	-382 -1097	-361 -845 -1087	-1162	-739 -920	-799 -875	-588 -920	-935*	-996* -1269
15	-1022	-1022	-871	-1173		-1208			-1162	-1132	-1087*
16	-1097	-1022			-1087	-1026	-906 -1147	-1208	-1117		-875
17	-1097	-1097	-871 -1173			-1208	-1056	-1178		-1162 -1253	-1132
18	-1060	-1097		-1173		-316 -1102 -1253				-1011	-1087*
19	-721 -909 -1060	-1022	-533 -947	-1022	-1238			-150 -1223	-135*	-1314	
20	-1060	-495 -1022	-683 -1060	-1022		-1208					

TABLE 2 (contd)

Velocities in the Crab Nebula (Blueshifts in km/sec)

COLUMN NUMBER X

ROW NUMBER Y	34	35	36	37	38	39	40	41	42	43	44
11	-1481	-1527	-1511	-1542					-1618	-1299	-1299*
12	-1466			-1178	-1299 -1466	-1299 -1542	-1436	-1405	-1436	-1405	
13	-376 -845 -1132 -1405	-392 -1147	-1117	-1238	-1117 -1193*	-1253 -1527			-950*	-890	-845 -1664
14	-708 -1026* -1269*	-860* -1056*	-1132*		-1026 -1299		-875* -1344	-860 -1072 -1360	-829* -950 -1147	-769* -905 -1087	-512 -769* -1329
15	-996 -1344	-1011*	-905 -1117	-875 -1360	-392 -769 -845	-739*			-663* -890	-618* -920	-437 -603* -1011
16	-1011	-1011*	-1072	-966	-890*	-739 -829 -905 -1026	-799* -1026*		-784* -1072	-739* -1064	-754*
17	-1072	-960	-920 -1011		-860	-799* -1132	-845*	-784	-784	-739* -875	-981*
18	-1102*	-1102	-769	-814 -1011	-875	-769* -950	-708* -890	-226 -739 -875	-226 -678	-648*	
19		-1132		-663	-663	-678	-618 -966	-573*	-542* -1162	-527 -1344	-437
20		-1041 -1299		-527	-542 -708	-422*	-422* -1056	-422* -603 -920 -1223	-392* -708 -935	-392	-407

TABLE 2 (contd)

Velocities in the Crab Nebula (Blueshifts in km/sec)

COLUMN NUMBER X

ROW NUMBER Y	45	46	47	48	49	50	51	52	53	54	55
11	-877*	-906* -1435	-994*	-1141	-1141	-1024 -1229	-1082	-760* -1141	-760*		-146 -613* -906
12	-848*	-848*	-848*	-936* -1347	-1082 -1347	-321 -613* -1141 -1317	-350 -643* -1141 -1317	-321 -701* -1024	-292* -731	-263* -672	-233 -989
13	-789* -1523	-760* -1435	-672* -1200 -1494	-467 -643* -906 -1317	-467* -936 -1333	-46 -1013	-379* -814	-321 -906 -1129	-536 -818	-555	-496
14	-721*	-683*	-608*	-458* -796*	-382* -909*	-345* -1097*	-382 -947	-909*	-984	-1135*	-1097
15	-458* -721* -1248	-683* -909* -1248*	-984* -1173*	-796* -1211*	-758* -1211*	-796* -1286	-195* -796*	-195* -758* -1135	-195* -834* -1211*	-270* -796* -1211	-270* -834*
16	-645 -984*		-796	-796*						-82 -1060	-120
17	-1135	-995*	-984*	-758 -1022	-495 -984*	-1135*	-458	-1097			
18			-1173	-758	-495	-758 -984	-984*	-1022	-1060	-1097	
19	-345*	-1173	-1173	-834 -1135	-834	-796				-1173	
20	-345*	-307* -1135	-1135		-871*		-909	-909	-947		-195

TABLE 2 (contd)

Velocities in the Crab Nebula (Blueshifts in km/sec)

COLUMN NUMBER X

ROW NUMBER Y	56	57	58	59	60	61	62	63	64	65	66
11	−146* −613. −877.	−146. −555. −906.	−29. −146. −555.	−117. −526.	−175. −848.	−204. −496.	−204.	−146.	−204.		
12	−146. −496. −701.	−146. −643.	−672.					−409.	−379.		
13	−87. −526. −1112.	−87.		−87.		−146.	−117.				
14	−608. −1060.	−495.	−7. −382. −570.	−7. −307.	−7.						
15	−307* −871*	−307* −533* −871.	−197. −664.	−197. −624.	−637.	−224. −704.	−184. −317.	−170.			
16		−120.	−157. −608.	−157.							
17	−45.										
18	−608. −871.	−645*	−645.	−645.	−683.	−645.					
19		−871.	−834.	−345.							
20			−120.	−120.							

Velocities in the Crab Nebula (Blueshifts in km/sec)

COLUMN NUMBER X

ROW NUMBER Y	1	2	3	4	5	6	7	8	9	10	11
21							-458.	-570. -758.	-345.	-345.	-796.
22									-382. -495.	-645.	-683.
23							-608.			-570.	-570.
24	-48.					-197.	-107.	-107.	-286.	-226. -583.	-167. -524. -613.
25											-107.
26											
27											
28											

TABLE 2 (contd)

Velocities in the Crab Nebula (Blueshifts in km/sec)

COLUMN NUMBER X

ROW NUMBER Y	12	13	14	15	16	17	18	19	20	21	22
21	-195. -721.	-157. -495.	-495.	-622.		-495. -909.	-458. -909.	-420. -947.	-420* -984.	-871.	-871.
22	-195. -608.	-120. -495. -758.	-45. -834.	-45.					-195.	-120. -909.	-157*
23	-570.	-120. -570.	-495.	-45. -495.	-7. -420. -834.	-45. -345. -495. -947.	-947.	-909.	-984.		-758.
24	-494. -673. -970.	-78. -494. -940.	-78. -494. -940.	-78. -286. -554.	-18. -197. -613.	-226. -1030.	-702.	-702.	-911.	-911.	-881.
25	-167. -583.	-137. -554.	-48. -643.	-18. -643.	-732.	-702.	-435. -762.	-792.	-792.	-821.	
26		-643.	-702.	-851.	-821.	-881.	-48. -881.	-48. -911.	-881.	-792.	-881.
27			-762.	-554. -851.	-702.	-18. -911.	-881.	-18.	-197.	-197.	-286. -732.
28			-286. -643.	-583.	-345. -762.	-256. -792.	-851.	-821.		-256.	-226. -583.

TABLE 2 (contd)

Velocities in the Crab Nebula (Blueshifts in km/sec)

COLUMN NUMBER X

ROW NUMBER Y	23	24	25	26	27	28	29	30	31	32	33
21	-947.	-947.	-947.	-1060.	-1056.	-981. -1102.	-966.				
22		-796.	-834.	-1022.						-981.	-45.
23	-871.	-796.	-758.	-721. -871.	-905.	-1087.		-1087.	-1087.	-1056.	-1072.
24	-821.	-851.	-940.		-762. -1059.	-732. -1059.	-762.	-613.			-1119.
25		-821.	-940.	-911.	-911.	-1059.	-792.		-702*	-732. -881.	-792.
26	-792.	-821.	-762.	-762. -1000.	-1030.	-940.	-18. -911.	-48. -762.	-137. -673.	-583.	-375. -524. -940.
27	-286. -762.	-286. -762.	-286. -702.	-435. -554.	-18. -375. -732.	-107. -256. -761.	-226. -792.	-375. -702.	-197. -494. -732.	-78. -169. -524. -762.	-524.
28	-197. -673.	-226. -673.	-613.	-226. -613.	-197. -345. -554.	-167. -435.	-48. -464.	-494.	-345.	-107. -464.	-226.

TABLE 2 (contd)

Velocities in the Crab Nebula (Blueshifts in km/sec)

COLUMN NUMBER X

ROW NUMBER Y	34	35	36	37	38	39	40	41	42	43	44
21		-537. -648.	-437. -633.	-452. -724.	-392. -542.	-361. -482.	-361* -754.	-196. -331*	-166. -437. -754.	-256. -769.	-135. -316.
22	-105. -875.	-211. -875*	-875*		-30* -166*	-90. -633.	-105* -678.	-105*	-135* -603*	-75.	-75. -376.
23	-166. -1026*	-166. -1072.	-196.	-15. -241.	-75. -181. -693. -829.	-166. -693. -829.	-75. -211.	-210.	-60. -467. -799.	-75. -392.	-45. -346.
24	-1059.	-1089.		-197. -495.	-197.	-78. -167. -345.	-345. -761.	-197. -673.	-226. -732.	-18. -226.	-48. -286.
25			-702.	-286. -613.	-256. -554.	-226. -494. -673. -851.	-226. -554. -851.	-167.	-226.	-78.	-137.
26	-524.	-495. -643.	-345. -613.	-345.	-316. -732.	-316. -762.	-78. -316.		-18.		
27	-405. -702.	-435.	-435. -702.	-435. -702.	-345. -762.	-48. -345.	-197.				
28	-226.	-197.	-137.	-78. -286.	-48.	-48.					

1983MNRAS.204..415C

TABLE 2 (contd)

Velocities in the Crab Nebula (Blueshifts in km/sec)

COLUMN NUMBER X

ROW NUMBER Y	45	46	47	48	49	50	51	52	53	54	55
21	-82. -345. -1022.	-307.	-307* -758.	-120. -758.	-82. -758.	-1022.	-1022.			-195.	-120.
22	-382. -570.	-570. -834.	-345. -608. -871.	-195. -533. -721.	-195. -721. -947.	-157. -1060.	-157. -1060.	-232. -1097.	-157. -721. -984.	-195.	-157.
23	-7. -570.			-196. -754.	-256. -557. -708. -799.	-196. -512. -814.	-181.	-241. -845.	-226. -860.	-256. -769.	-166. -754*
24	-108. -256. -553.	-48. -256.	-48. -404.	-48.		-18. -673.	-613.	-316. -583. -673.	-226. -583.	-316. -583. -821.	-286. -554. -762.
25		-197.			-107.			-554.	-583.	-256. -583.	-316. -554.
26	-137.	-78.	-107.	-167.	-78.						
27											
28											

TABLE 2 (contd)

Velocities in the Crab Nebula (Blueshifts in km/sec)

COLUMN NUMBER X

ROW NUMBER Y	56	57	58	59	60	61	62	63	64	65	66
21	-157.	-82.	-45.		-45.						
22	-570.	-82.		-7.	-157.						
23	-166. -497.		-754.	-422. -739. -875.							
24	-226. -554. -792.	-316. -702. -851.	-375. -583. -792.	-435. -792. -911.	-197. -316. -851.	-167. -345. -792.	-613.	-613.	-554.		
25	-583.	-524.	-464. -821.	-792.							
26											
27											
28											

Table 1. Velocities in the Crab Nebula (redshifts).

Table 2. Velocities in the Crab Nebula (blueshifts).

Note to Tables. These tables list the velocities extracted from the data brick referred to in the text. Each row corresponds to an E-W position of the spectrograph slit on the Crab Nebula, and each column a N-S increment. Rows and columns are numbered from the NE corner, and are related to right ascension and declination by the formulae in Section 2. In each pixel numbers represent the radial velocity (in km s^{-1}) of a peak of emission of the λ5007 spectral line of [OIII]. Receding (positive) velocities are entered in Table 1 and approaching (negative) velocities in Table 2. The velocities of bright features are followed by asterisks.